Supplementary Material S1

Characteristic examples of solid boundary classification on the ports' waterfronts for the determination of partial/full wave reflection regimes in Model B's domains.

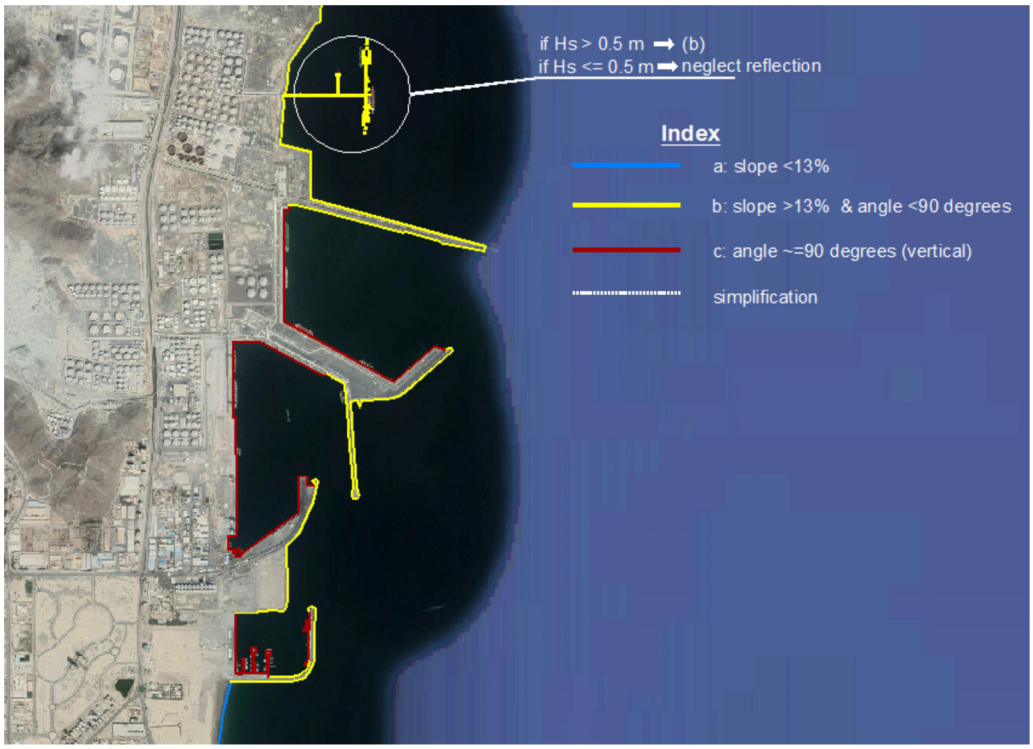

Figure S1.1 Port of Fujairah

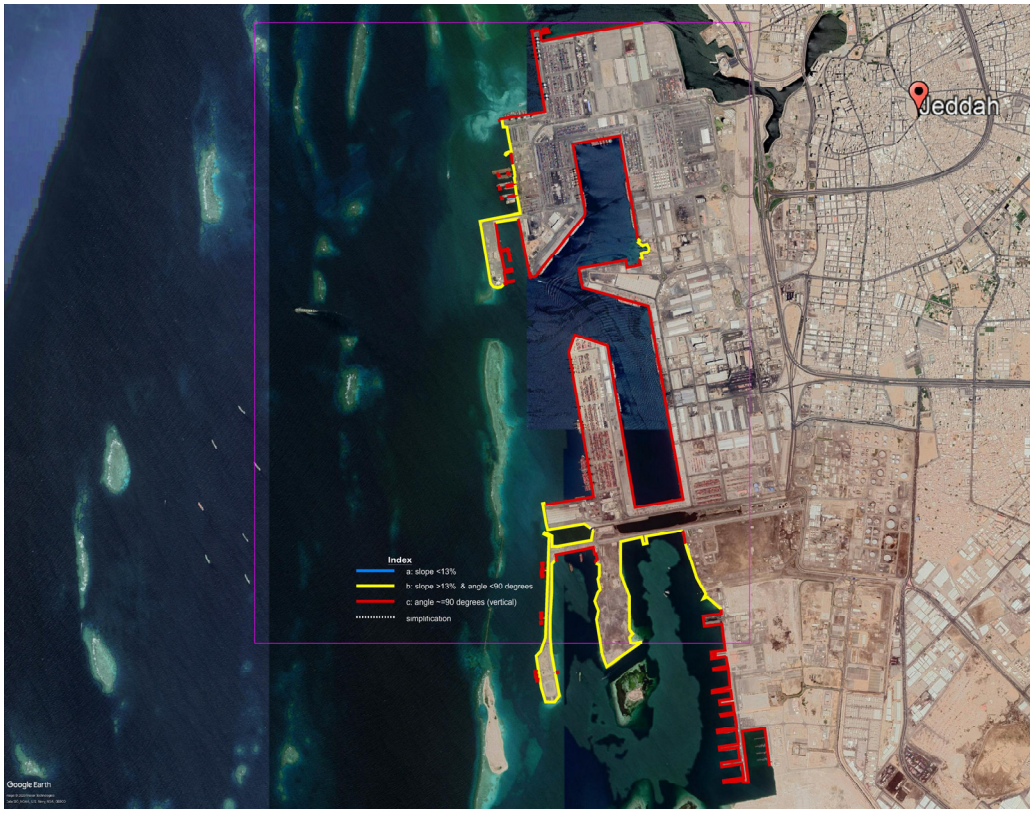

Figure S1.2 Port of Jeddah

Figure S1.3 Port of Colombo

Figure S1.4 Port of Cartagena

Figure S1.5 Port of Piraeus

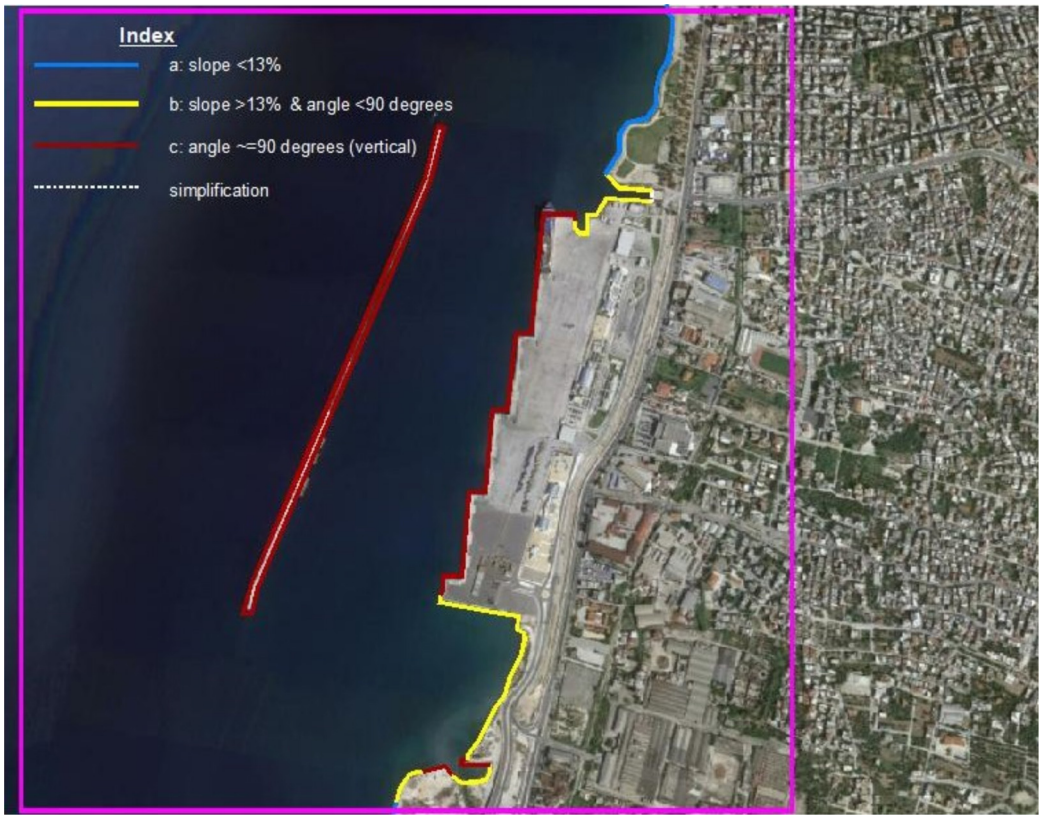

Figure S1.6 Port of Patra

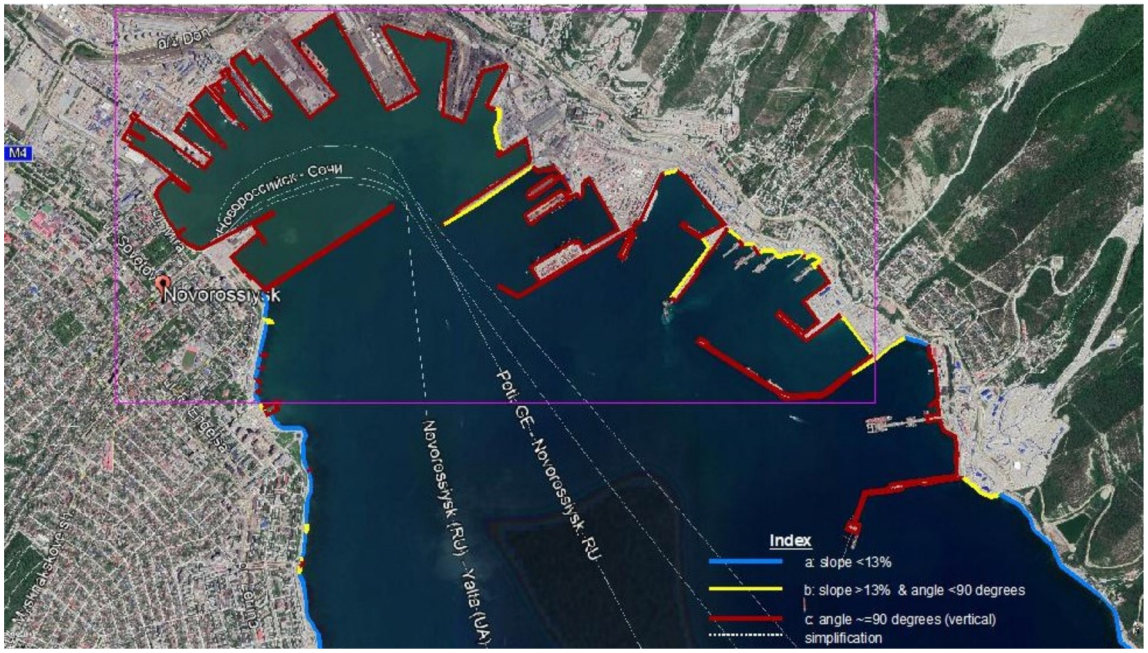

Figure S1.7 Port of Novorossiysk

Figure S1.8 Port of Ijmuiden

Supplementary Material S2

Characteristic details and depiction of the Accu-Waves OFP schematics of WFS model execution *in tandem* with patrimonial (external) and produced (internal) data flow.

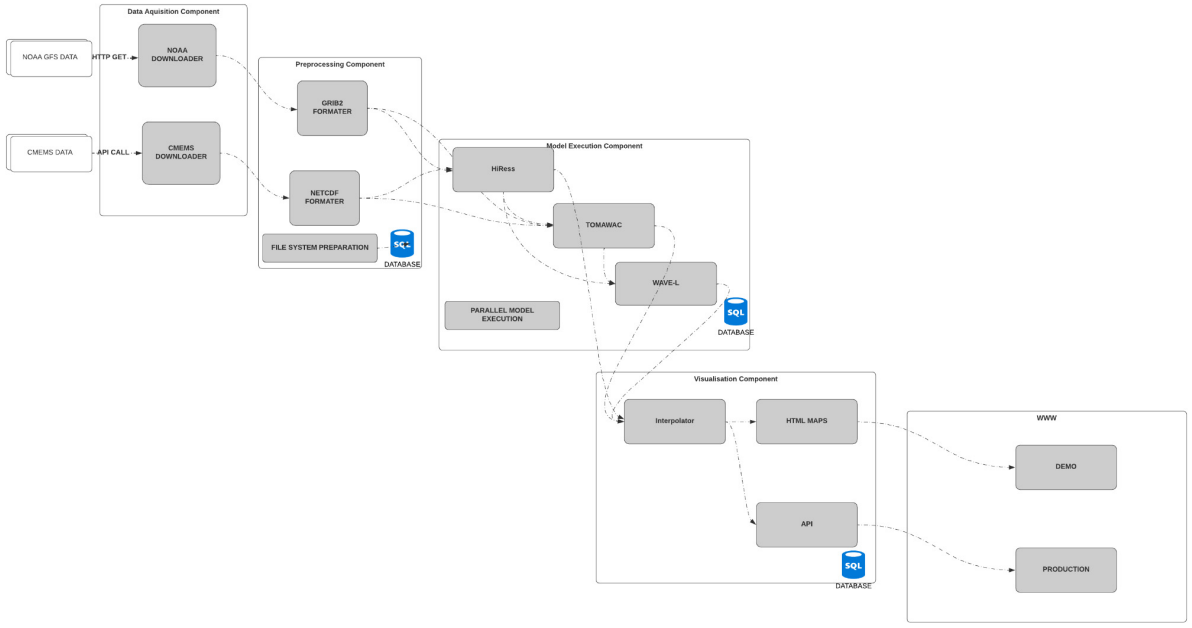

Figure S2.1. Detailed depiction of Accu-Waves system architecture.

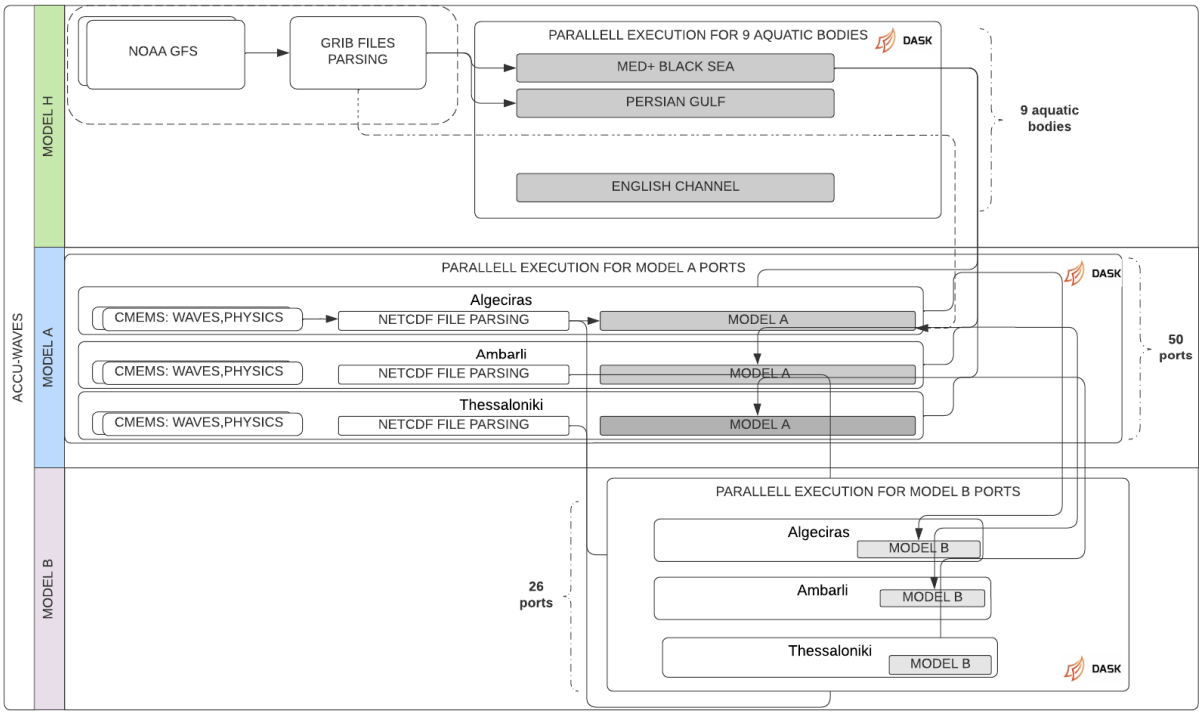

Figure S2.2 Schematics of the parallelization procedure of the Accu-Waves OFP computational tasks and codes' execution, and the WFS model runs.

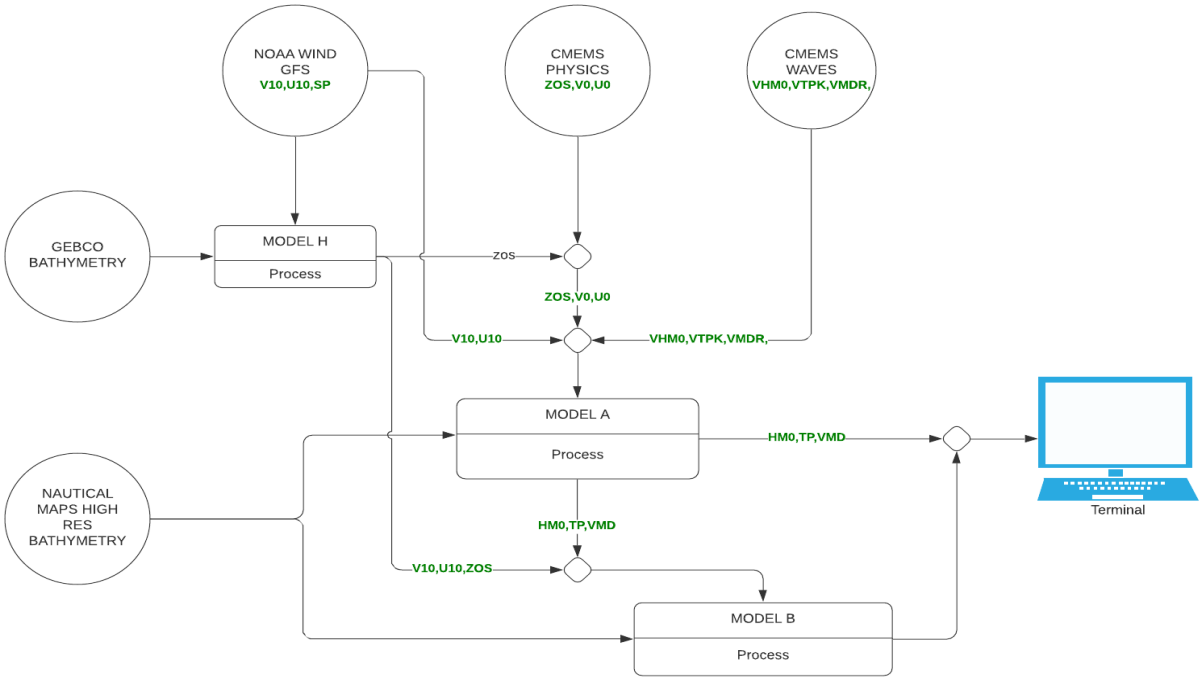

Figure S2.3. Schematics of model Accu-Waves OFP integration execution course and interaction of WFS model results. Parameters as written in the data-exchange *Python* coding system include: Significant Wave Height by CMEMS and Model A, VHMO and HMO, respectively; Peak Spectral Wave Period by CMEMS and Model A, VTPK and TP, respectively; Mean Wave Propagation Direction by CMEMS and Model A, VMDR and VMD, respectively; Meridional and Zonal Barotropic Current Speed components by either Model H or CMEMS, VO and UO; Mean Sea Level Elevation due to meteorological forcing and astronomical tides by either Model H or CMEMS, ZOS; Meridional and Zonal Wind Speed components by NOAA, V10 and U10. NOAA and CMEMS forecasts' data are provided freely for research purposes.

Supplementary Material S3

Figures of characteristic results by simulations with Model A in 49 globally significant ports are provided. All simulations refer to moderate, rough, and very rough wave conditions and highly detailed depictions of the wave-induced agitation in the areas surrounding the ports (Model A).

Scenarios	H_s (m)	T_p (s)	ϕi (˚)	Wind Speed	
				W_x (m/s)	W_y (m/s)
A#1	2.5	6.75	135	8.49	-8.49
A#2	5.5	11.0	135	17.68	-17.68

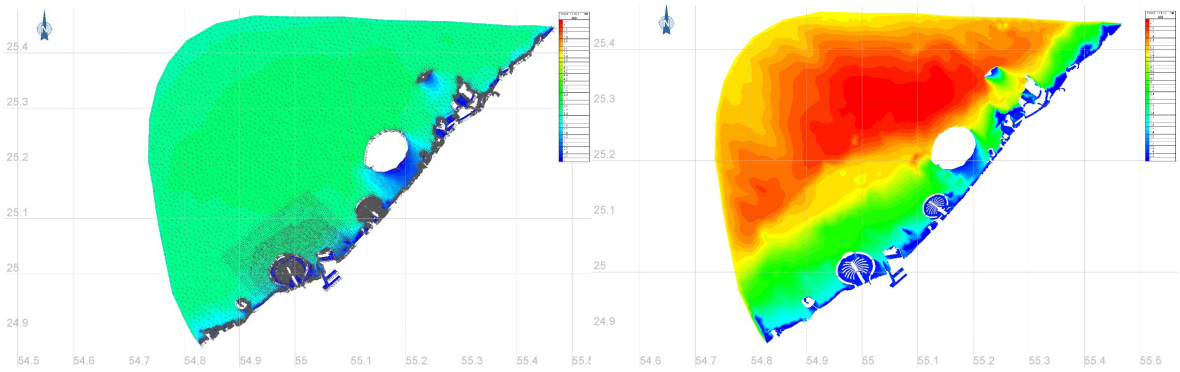

Figure S3.1. Characteristic operational WFS results of H_{mo} (m) by Model A in **Jebel Ali** (UAE, Persian Gulf; no. 2 of Table 1) port during W-NW sector moderate and very rough wave conditions, respectively. Scenarios A#1 (left) and A#2 (right).

Scenarios	H_s (m)	T_p (s)	ϕi (˚)	Wind Speed	
				W_x (m/s)	W_y (m/s)
A#1	1.80	4.5	225	-7.07	-7.07
A#2	3.80	10	225	-14.14	-14.14

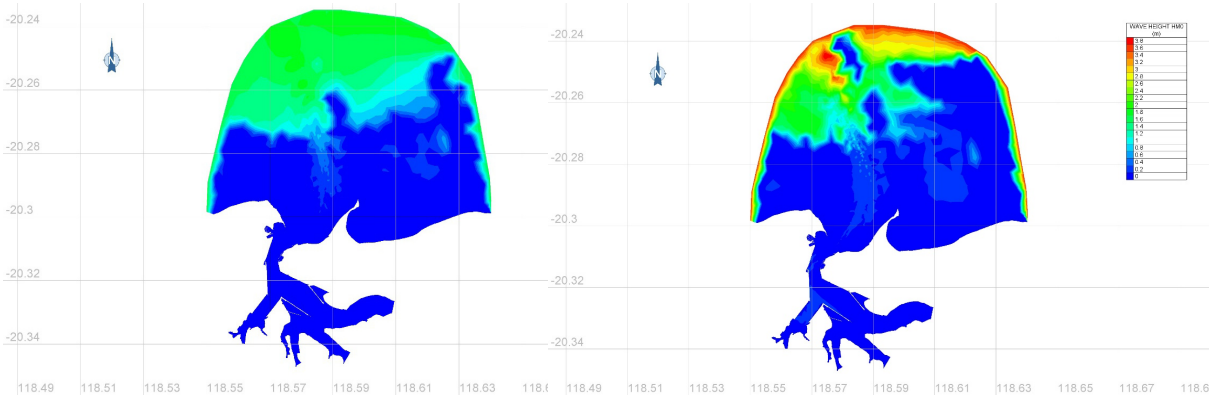

Figure S3.2. Characteristic operational WFS results of H_{mo} (m) by Model A in **Port Hedland** (Australia, Indian Ocean; no. 4 of Table 1) port during N-NE sector moderate and rough wave conditions, respectively. Scenarios A#1 (left) and A#2 (right).

Scenarios	H_s (m)	T_p (s)	ϕi (˚)	Wind Speed

				W_x (m/s)	W_y (m/s)
A#1	3.80	10	120	12.99	-7.5
A#2	1.80	4.5	90	10	0

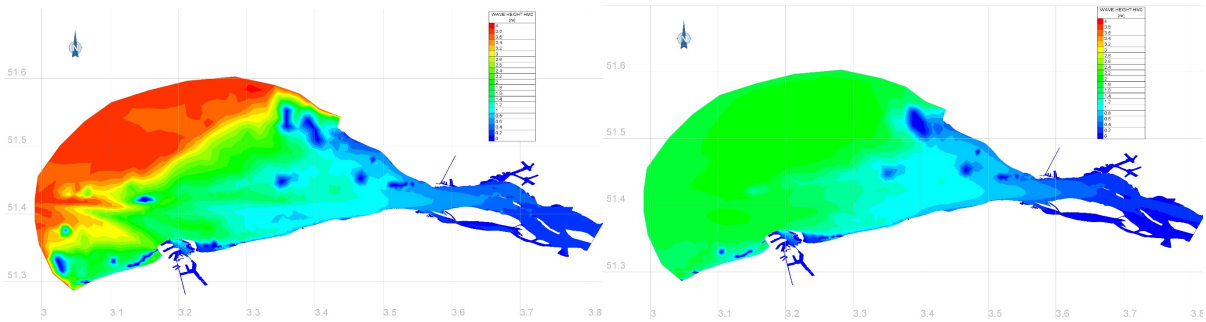

Figure S3.3. Characteristic operational WFS results of H_{mo} (m) by Model A in **Antwerp** (Belgium, North Sea; no. 5 of Table 1) port during W-NW and W sectors rough and moderate wave conditions, respectively. Scenarios A#1 (left) and A#2 (right).

Scenarios	H_s (m)	T_p (s)	ϕi (˚)	**Wind Speed**	
				W_x (m/s)	W_y (m/s)
A#1	2.5	6.75	315	-8.48	8.48
A#2	5.5	11.0	315	-17.68	17.68

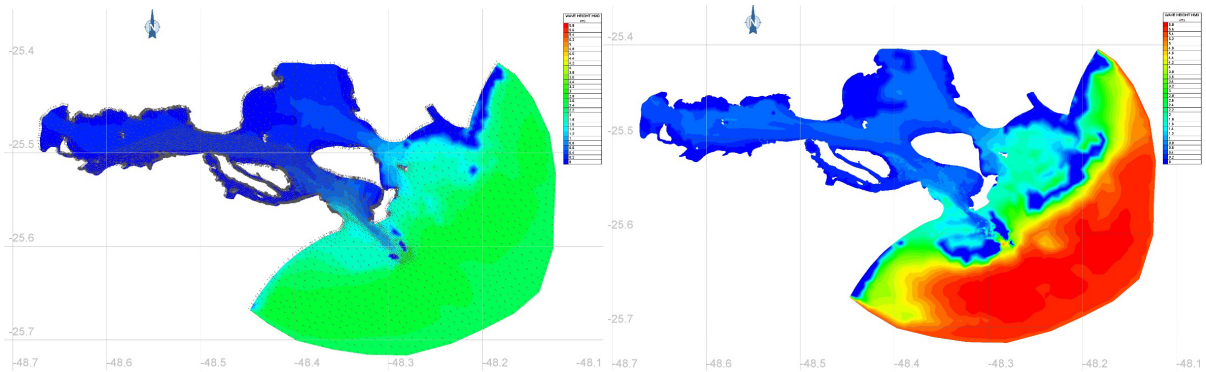

Figure S3.4. Characteristic operational WFS results of H_{mo} (m) by Model A in **Paranagua** (Brazil, Southwestern Atlantic Ocean; no. 6 of Table 1) port during SE sector moderate and very rough wave conditions, respectively. Scenarios A#1 (left) and A#2 (right).

Scenarios	H_s (m)	T_p (s)	ϕi (˚)	**Wind Speed**	
				W_x (m/s)	W_y (m/s)

A#1	2.5	6.75	315	-8.48	8.48
A#2	5.5	11	315	-8.48	8.48

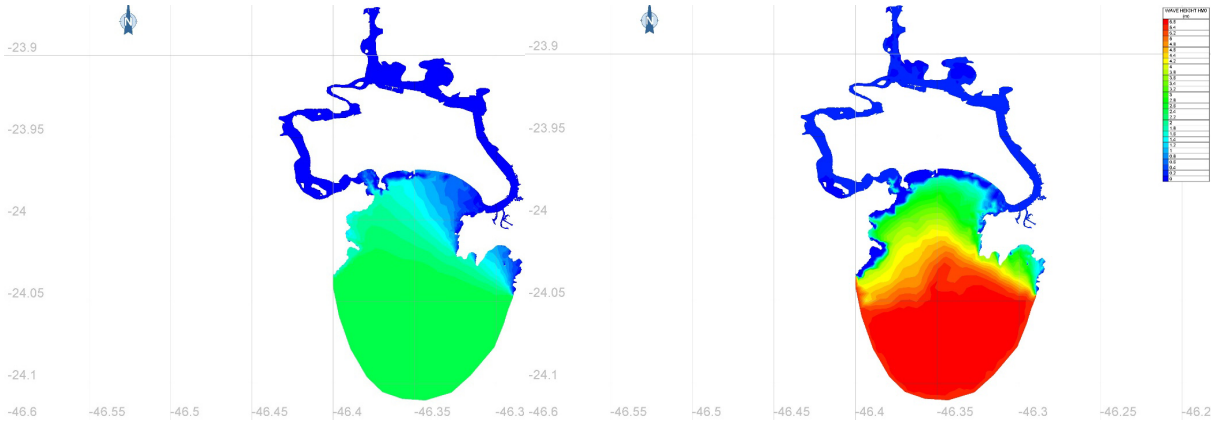

Figure S3.5. Characteristic operational WFS results of H_{mo} (m) by Model A in **Santos** (Brazil, Southwestern Atlantic Ocean; no. 7 of Table 1) port during SE sector moderate and very rough wave conditions, respectively. Scenarios A#1 (left) and A#2 (right).

Scenarios	**H_s (m)**	**T_p (s)**	**ϕi (˚)**	**Wind Speed**		**SLE (m)**
				W_x (m/s)	**W_y (m/s)**	
A#1	2.5	6.75	135	8.49	-8.49	0
A#2	5.5	11.0	135	17.68	-17.68	3.5

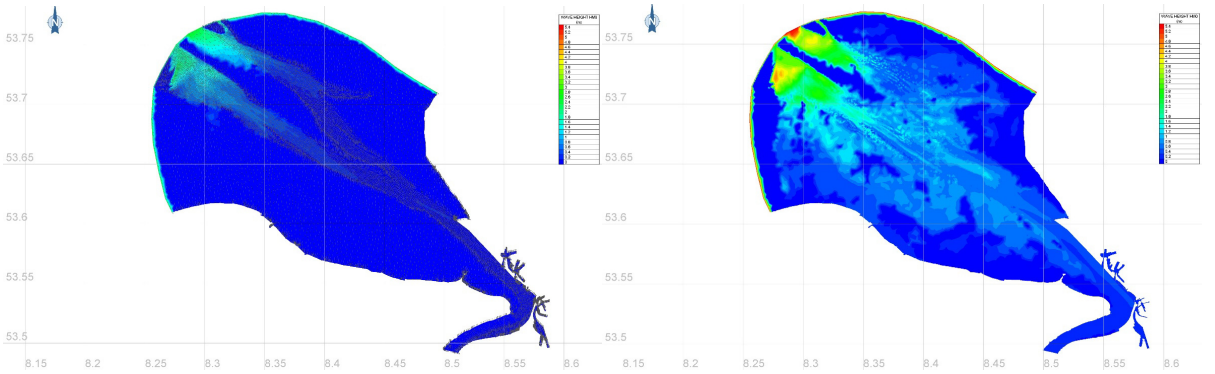

Figure S3.6. Characteristic operational WFS results of H_{mo} (m) by Model A in **Bremerhaven** (Germany, North Sea; no. 10 of Table 1) port during NW sector moderate and very rough wave conditions, respectively. Scenarios A#1 (left) and A#2 (right).

Scenarios	**H_s (m)**	**T_p (s)**	**ϕi (˚)**	**Wind Speed**		**SLE (m)**
				W_x (m/s)	**W_y (m/s)**	
A#1	1.8	4.5	135	7.07	-7.07	+0

A#2	3.8	10	135	14.14	-14.14	+3.5

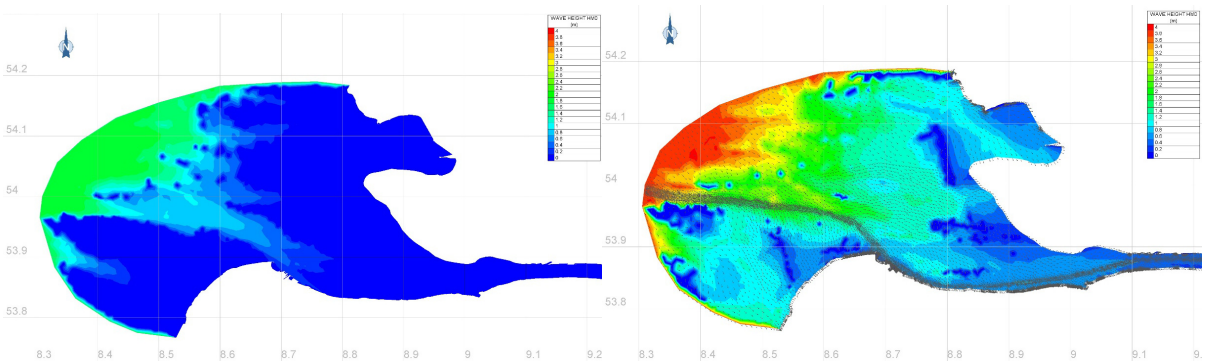

Figure S3.7. Characteristic operational WFS results of H_{mo} (m) by Model A in **Hamburg** (Germany, North Sea; no. 11 of Table 1) port during NW sector moderate and rough wave conditions, respectively. Scenarios A#1 (left) and A#2 (right).

Scenarios	**H_s (m)**	**T_p (s)**	**ϕi (˚)**	**Wind Speed**	
				W_x (m/s)	**W_y (m/s)**
A#1	1.80	4.5	225	-7.07	-7.07
A#2	3.80	10	270	-15	0

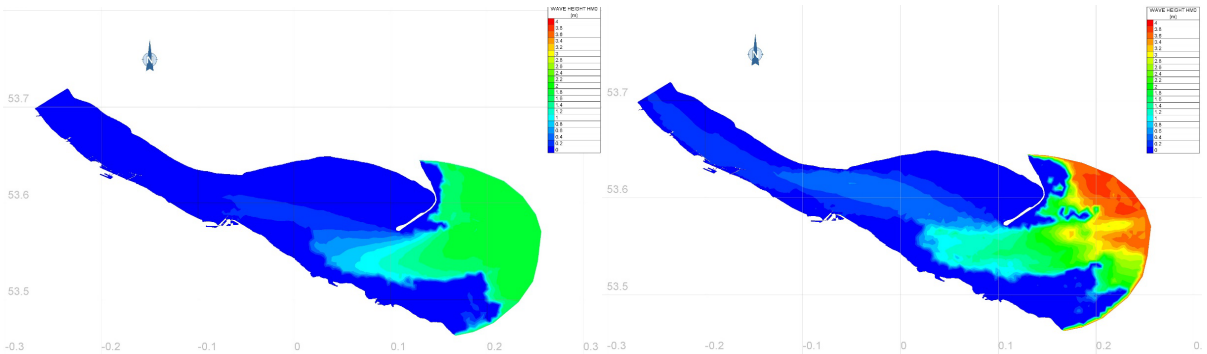

Figure S3.8. Characteristic operational WFS results of H_{mo} (m) by Model A in **Immingham** (UK, North Sea; no. 15 of Table 1) port during NE and E sectors moderate and rough wave conditions, respectively. Scenarios A#1 (left) and A#2 (right).

Scenarios	**H_s (m)**	**T_p (s)**	**ϕi (˚)**	**Wind Speed**	
				W_x (m/s)	**W_y (m/s)**
A#1	5.5	11	315	-17.68	17.68
A#2	2.5	6.75	45	8.49	8.49

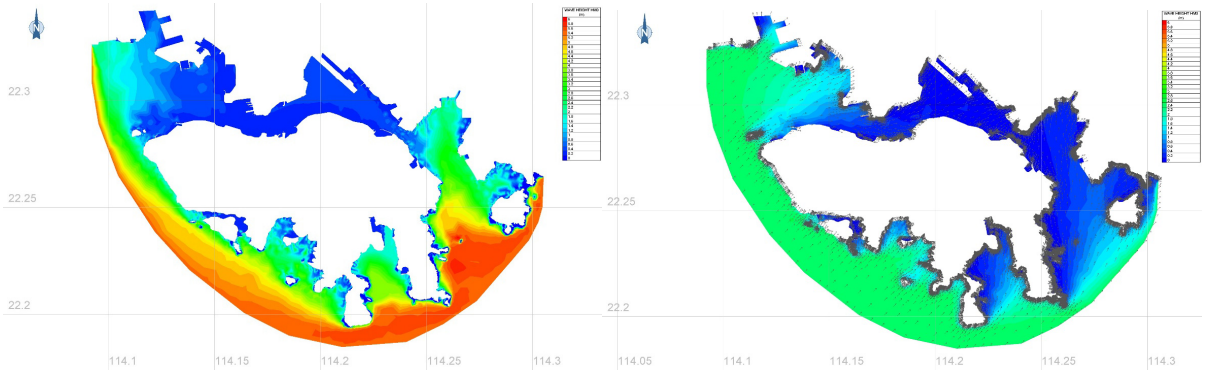

Figure S3.9. Characteristic operational WFS results of H_{mo} (m) by Model A in **Hong Kong** (China, Yellow Sea, West Pacific Ocean; no. 19 of Table 1) port during SE and SW sectors very rough and moderate wave conditions, respectively. Scenarios A#1 (left) and A#2 (right).

Scenarios	H_s (m)	T_p (s)	ϕi (˚)	Wind Speed	
				W_x (m/s)	W_y (m/s)
A#1	3.80	10	120	7.5	-13
A#2	3.80	10	180	0	-15

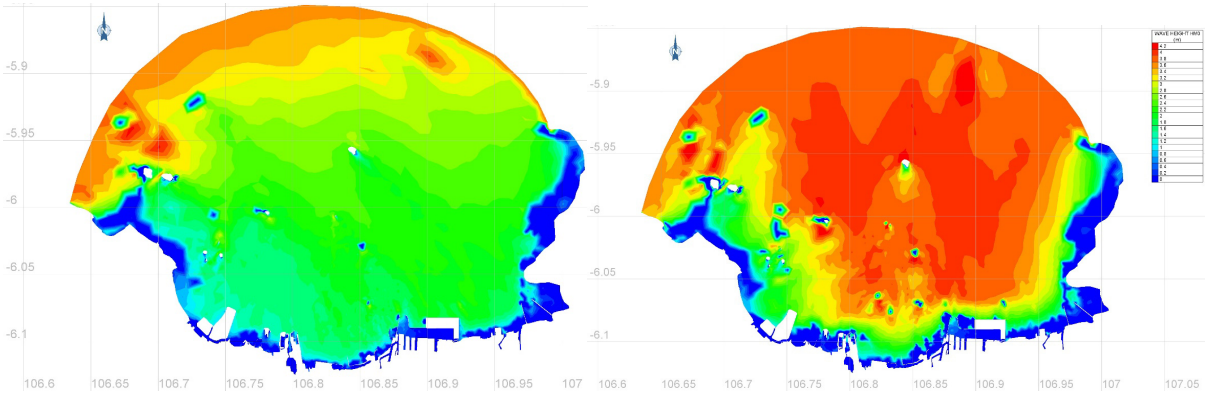

Figure S3.10. Characteristic operational WFS results of H_{mo} (m) by Model A in **Jakarta** (Indonesia, Java Sea; no. 20 of Table 1) port during NW and N sectors rough wave conditions, respectively. Scenarios A#1 (left) and A#2 (right).

Scenarios	H_s (m)	T_p (s)	ϕi (˚)	Wind Speed	
				W_x (m/s)	W_y (m/s)
A#1	2.5	6.75	45	10.6	10.6
A#2	5.5	11.0	45	17.67	17.67

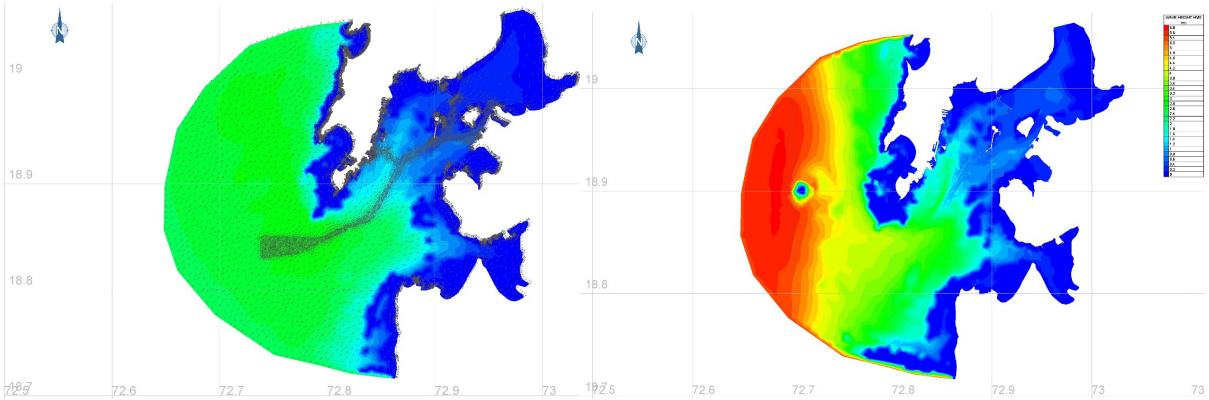

Figure S3.11. Characteristic operational WFS results of H_{mo} (m) by Model A in **Mumbai** (India, Arabian Sea; no. 23 of Table 1) port during SW sector moderate and very rough wave conditions. Scenarios A#1 (left) and A#2 (right).

Scenarios	H_s (m)	T_p (s)	ϕi (˚)	Wind Speed	
				W_x (m/s)	W_y (m/s)
A#1	2.5	6.75	75	14.48	3.88
A#2	5.5	11	75	24.14	6.47

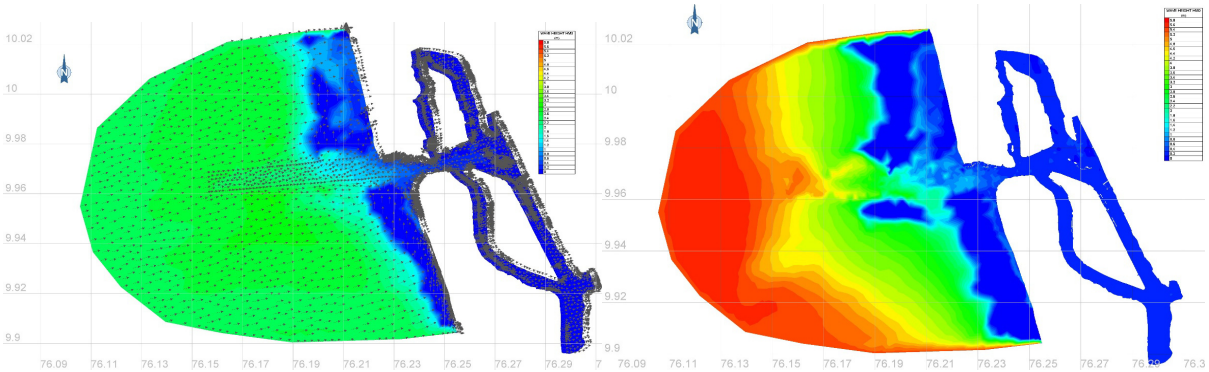

Figure S3.12. Characteristic operational WFS results of H_{mo} (m) by Model A in **Cochin** (India, Arabian Sea – Laccadive Sea – Indian Ocean sea-route; no. 24 of Table 1) port during W-SW sector moderate and very rough wave conditions. Scenarios A#1 (left) and A#2 (right).

Scenarios	H_s (m)	T_p (s)	ϕi (˚)	Wind Speed	
				W_x (m/s)	W_y (m/s)
A#1	2.5	6.75	20	4.10	11.27
A#2	5.5	11	20	8.55	23.49

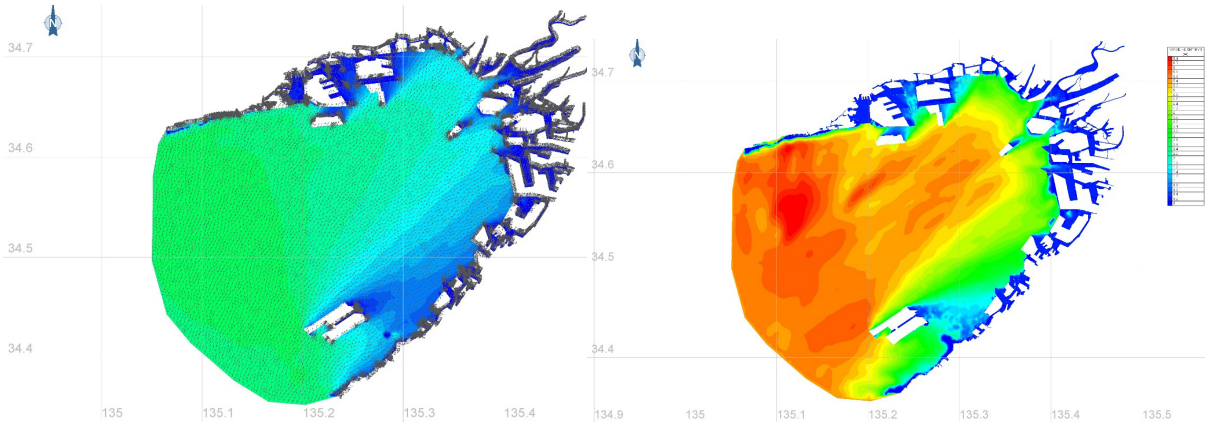

Figure S3.13. Characteristic operational WFS results of H_{mo} (m) by Model A in **Osaka** and **Kobe** (Japan, West Pacific Ocean; no. 26 & 28 of Table 1) ports during S-SW sector moderate and very rough wave conditions. Scenarios A#1 (left) and A#2 (right).

Scenarios	H_s (m)	T_p (s)	ϕi (˚)	Wind Speed	
				W_x (m/s)	W_y (m/s)
A#1	3.1	4.5	40	3.5	12.0
A#2	0.0	0.0	0	16.5	19.1

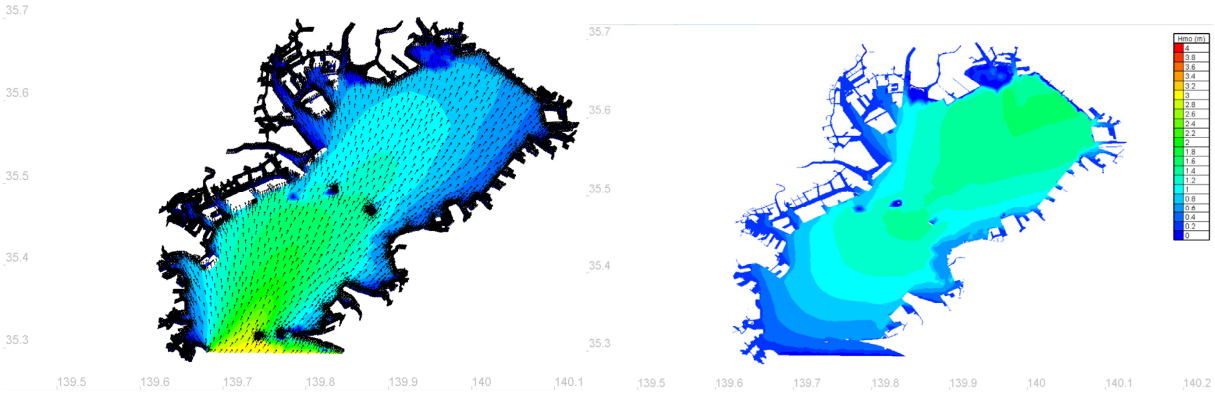

Figure S3.14. Characteristic operational WFS results of H_{mo} (m) by Model A in **Tokyo (Gulf)** (Japan, West Pacific Ocean) port during SW-S sector rough wave and outer-bay dead calm (only wind-wave generation inside Tokyo Gulf; no. 27 of Table 1) conditions, respectively. Scenarios A#1 (left) and A#2 (right).

Scenarios	H_s (m)	T_p (s)	ϕi (˚)	Wind Speed	
				W_x (m/s)	W_y (m/s)
A#1	1.8	4.5	45	7.07	7.07
A#2	3.8	10.0	45	14.14	14.14

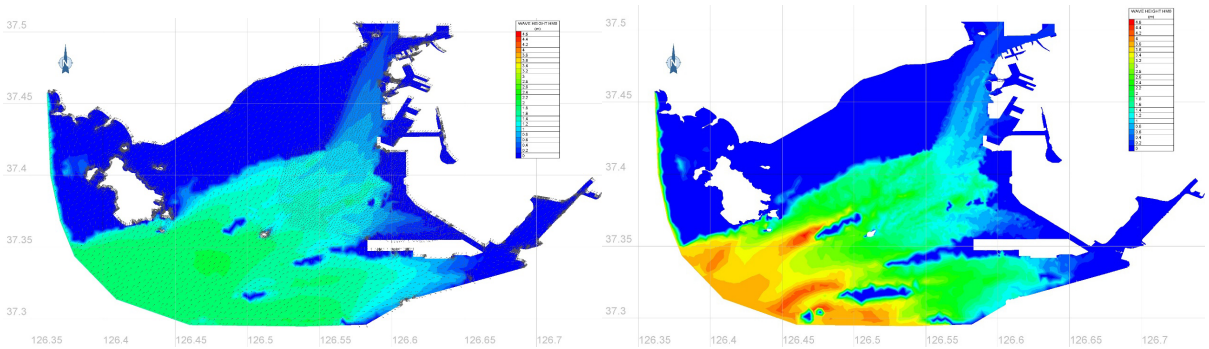

Figure S3.15. Characteristic operational WFS results of H_{mo} (m) by Model A in **Incheon** (South Korea, Yellow Sea; no. 30 of Table 1) port during SW sector moderate and rough wave conditions. Scenarios A#1 (left) and A#2 (right).

Scenarios	H_s (m)	T_p (s)	ϕi (˚)	Wind Speed	
				W_x (m/s)	W_y (m/s)
A#1	1.8	4.5	45	7.07	7.07
A#2	3.8	10.0	45	14.14	14.14

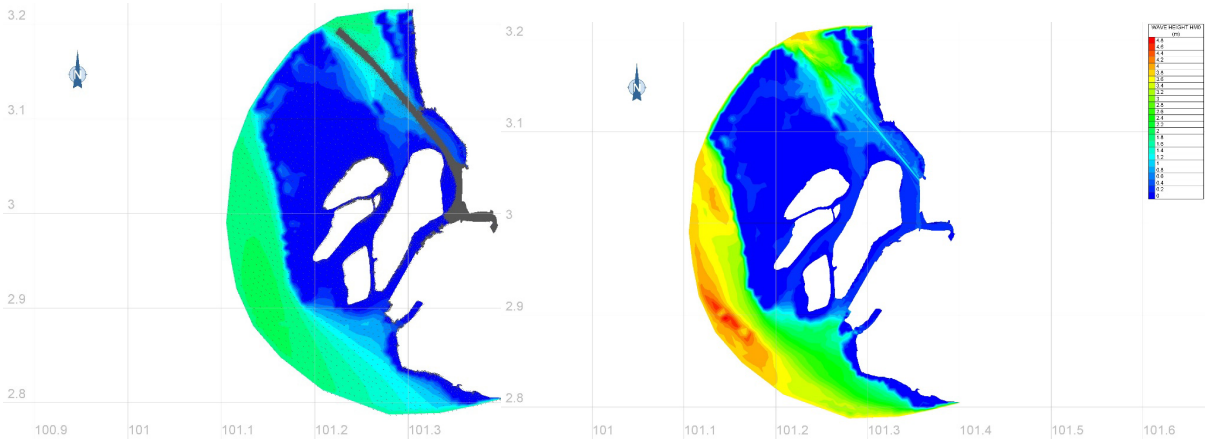

Figure S3.16. Characteristic operational WFS results of H_{mo} (m) by Model A in **Port Klang** (Malaysia, Malacca Strait, Indian Ocean; no. 33 of Table 1) during SW sector moderate and rough wave conditions. Scenarios A#1 (left) and A#2 (right).

Scenarios	H_s (m)	T_p (s)	ϕi (˚)	Wind Speed	
				W_x (m/s)	W_y (m/s)
A#1	2.5	6.75	0	0.0	12.0
A#2	5.5	11.0	315	-17.68	17.68

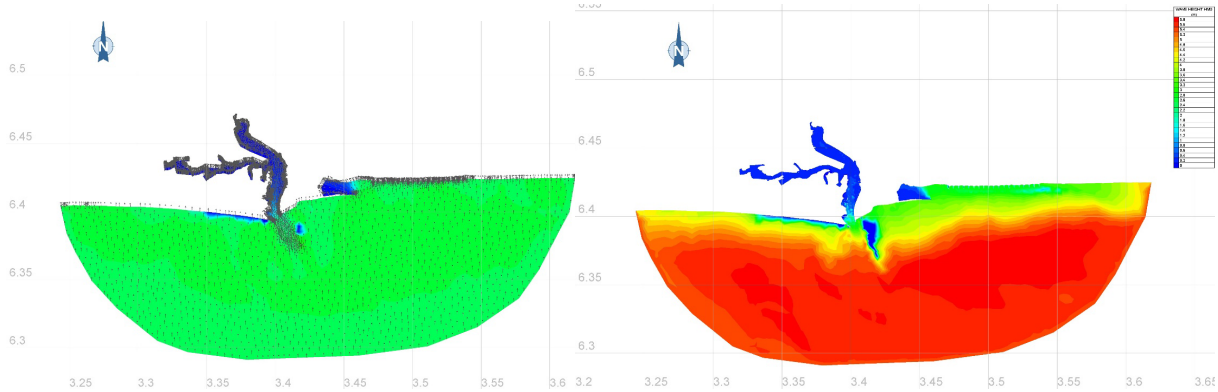

Figure S3.17. Characteristic operational WFS results of H_{mo} (m) by Model A in **Lagos** (Nigeria, East-central Atlantic Ocean; no. 34 of Table 1) port during S and SE sector moderate and very rough wave conditions. Scenarios A#1 (left) and A#2 (right).

Scenarios	H_s (m)	T_p (s)	ϕi (˚)	Wind Speed	
				W_x (m/s)	W_y (m/s)
A#1	1.8	4.5	135	7.07	-7.07
A#2	3.8	10	135	14.14	-14.14

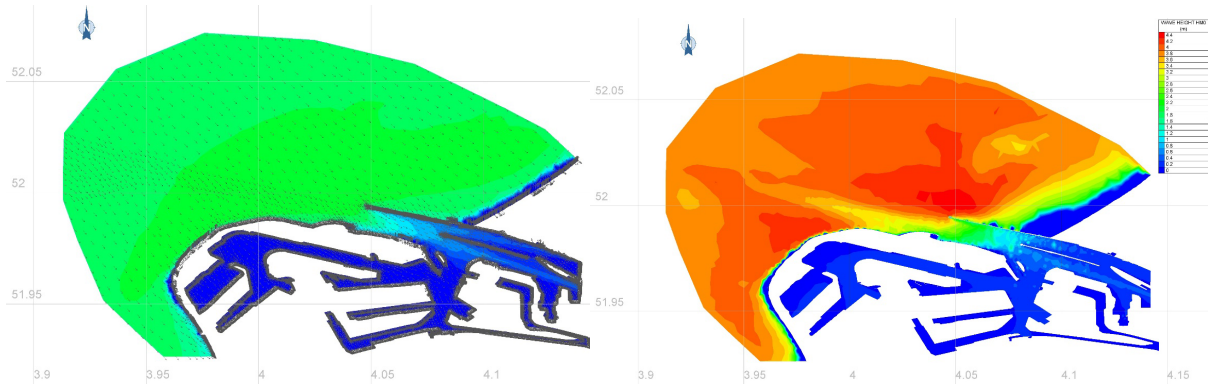

Figure S3.18. Characteristic operational WFS results of H_{mo} (m) by Model A in **Maasvlakte Rotterdam** (Netherlands, North Sea; no. 36 of Table 1) port during NW sector moderate and rough wave conditions. Scenarios A#1 (left) and A#2 (right).

Scenarios	H_s (m)	T_p (s)	ϕi (˚)	Wind Speed	
				W_x (m/s)	W_y (m/s)
A#1	1.8	4.5	270	-10.0	0.0
A#2	3.8	10.0	270	-20.0	0.0

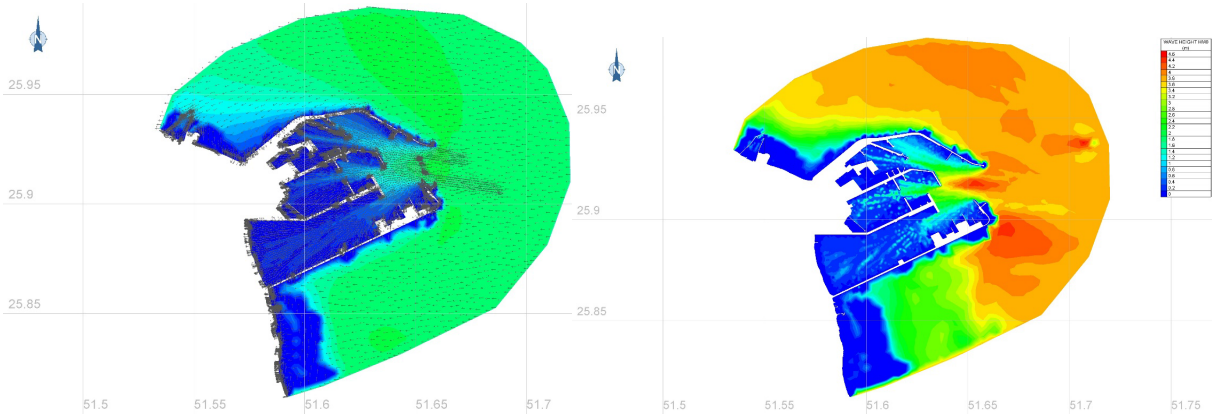

Figure S3.19. Characteristic operational WFS results of H_{mo} (m) by Model A in **Ras Lafan** (Qatar, Persian Gulf; no. 38 of Table 1) port during W sector moderate and rough wave conditions. Scenarios A#1 (left) and A#2 (right).

Scenarios	H_s (m)	T_p (s)	ϕi (˚)	Wind Speed	
				W_x (m/s)	W_y (m/s)
A#1	1.8	4.5	270	-10.0	0.0
A#2	1.8	4.5	0	0.0	-10.0

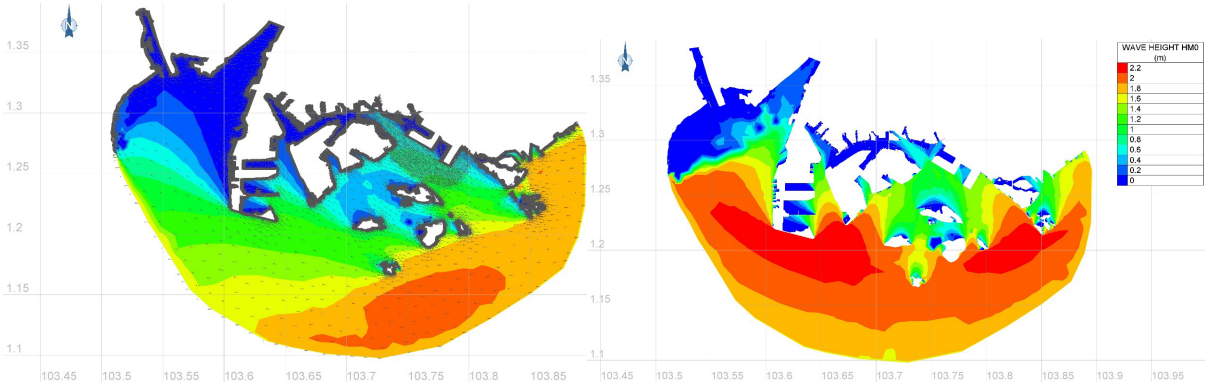

Figure S3.20. Characteristic operational WFS results of H_{mo} (m) by Model A in **Singapore** (South China Sea; no. 42 of Table 1) port during W and N sector moderate wave conditions. Scenarios A#1 (left) and A#2 (right).

Scenarios	H_s (m)	T_p (s)	ϕi (˚)	Wind Speed	
				W_x (m/s)	W_y (m/s)
A#1	1.8	4.5	0	0	10
A#2	3.8	10	0	0	20

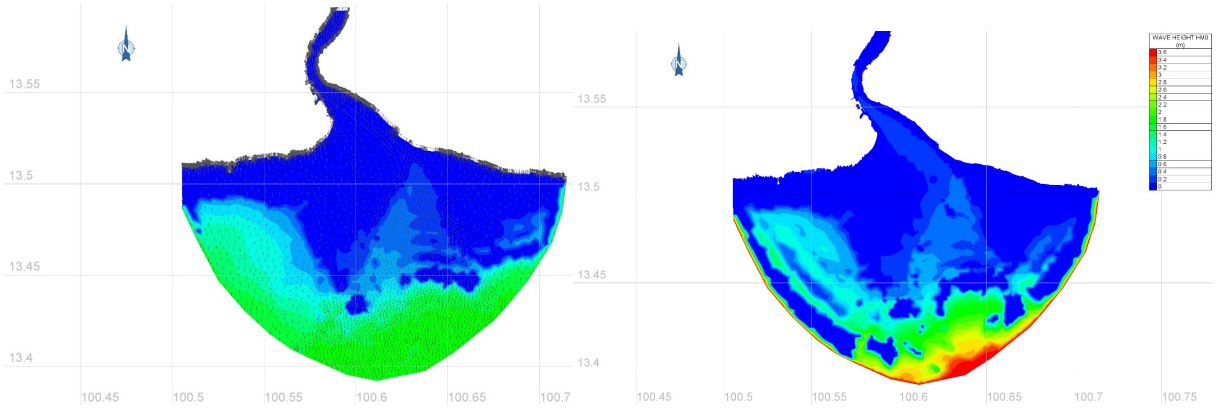

Figure S3.21. Characteristic operational WFS results of H_{mo} (m) by Model A in **Bangkok** (Thailand, Gulf of Thailand; no. 43 of Table 1) port during N sector moderate and rough wave conditions. Scenarios A#1 (left) and A#2 (right).

Scenarios	H_s (m)	T_p (s)	ϕi (˚)	Wind Speed	
				W_x (m/s)	W_y (m/s)
A#1	5.5	11.0	90	25.0	0.0
A#2	5.5	11.0	0	0.0	25.0

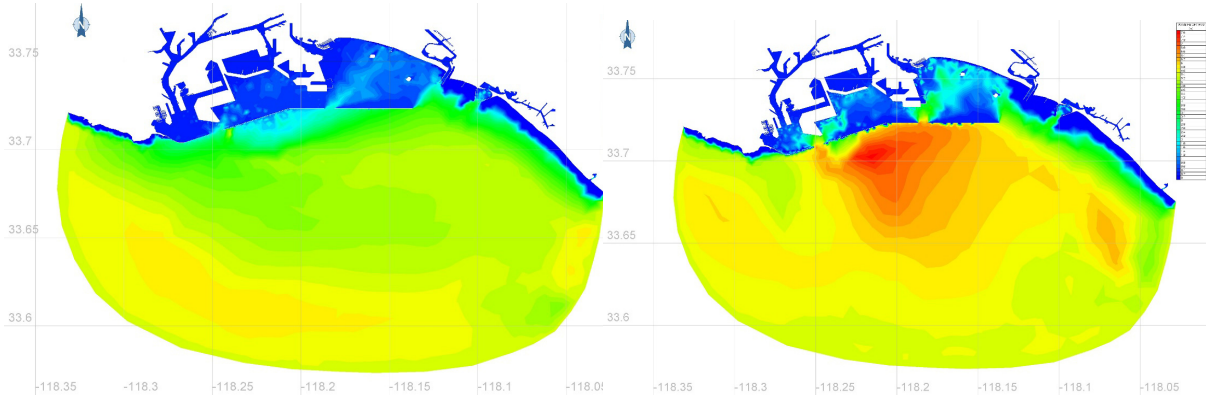

Figure S3.22. Characteristic operational WFS results of H_{mo} (m) by Model A in **Los Angeles** (USA, East Pacific; no. 46 of Table 1) port during W and N sector very rough wave conditions. Scenarios A#1 (left) and A#2 (right).

Scenarios	H_s (m)	T_p (s)	ϕi (˚)	Wind Speed	
				W_x (m/s)	W_y (m/s)
A#1	2.8	6.75	270	-13.0	0.0
A#2	3.2	10.0	315	-9.19	-9.19

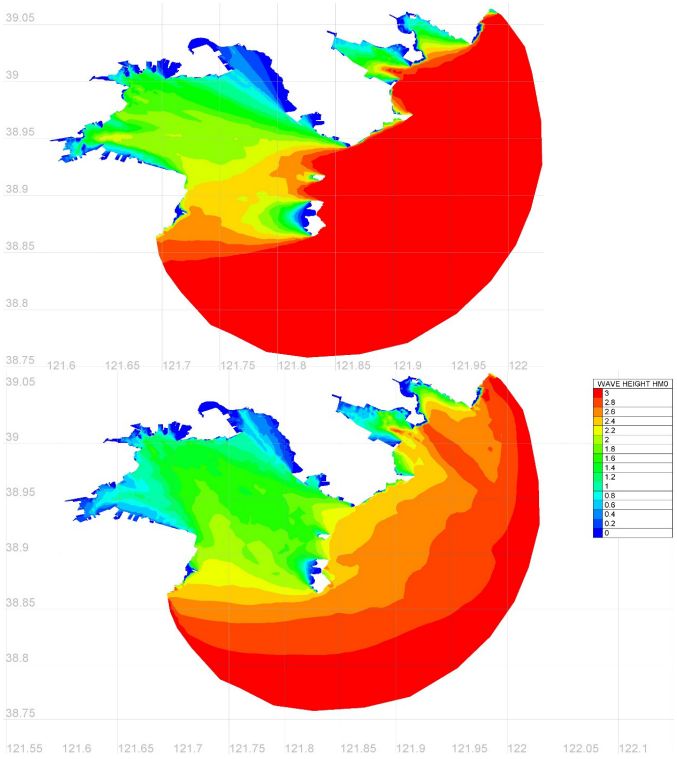

Figure S3.23. Characteristic operational WFS results of H_{mo} (m) by Model A in **Dalian 1 & 2** (China, Yellow Sea; no. 47 and 49 of Table 1) port during E and SE sector moderate and rough wave conditions. Scenarios A#1 (left) and A#2 (right).

Scenarios	H_s (m)	T_p (s)	ϕi (˚)	Wind Speed	
				W_x (m/s)	W_y (m/s)
A#1	2.5	6.75	315	-8.49	8.49
A#4	5.5	11	270	-25	0

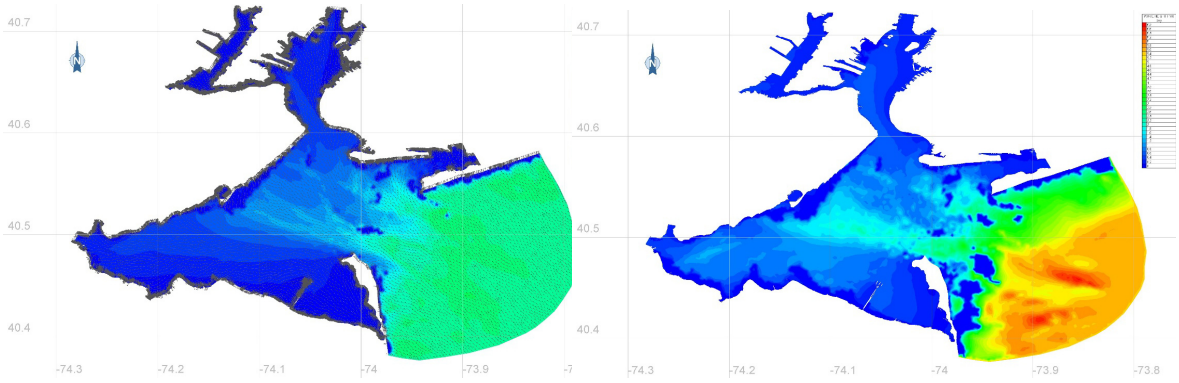

Figure S3.24. Characteristic operational WFS results of H_{mo} (m) by Model A in **New York** (USA, Northwest Atlantic Ocean; no. 48 of Table 1) port during SE and E sector moderate and very rough wave conditions. Scenarios A#1 (left) and A#2 (right).

Scenarios	H_s (m)	T_p (s)	ϕi (˚)	Wind Speed	
				W_x (m/s)	W_y (m/s)
A#1	5.5	11.0	315	-17.68	17.68
A#2	3.8	10.0	225	-14.14	-14.14

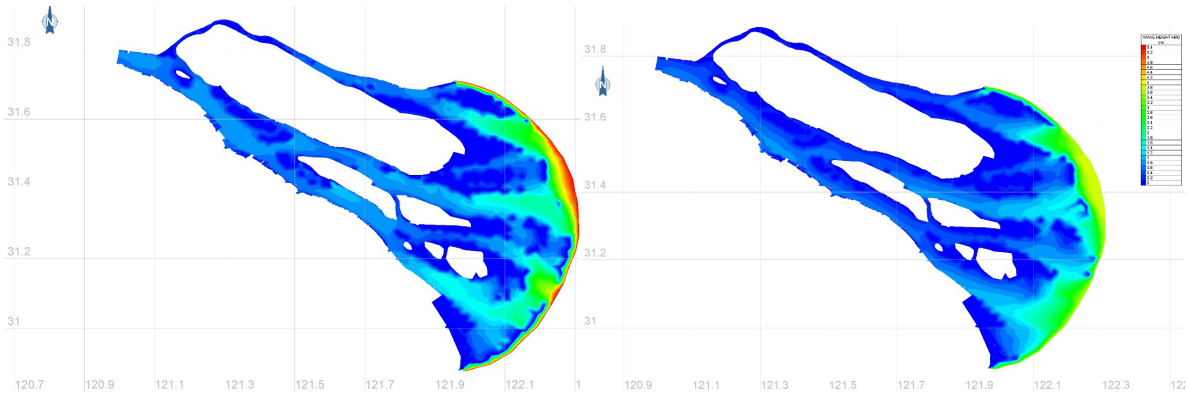

Figure S3.25. Characteristic operational WFS results of H_{mo} (m) by Model A in **Shanghai** (China, Yellow Sea; no. 50 of Table 1) port during SE and NE sector very rough and rough wave conditions. Scenarios A#1 (left) and A#2 (right).

Scenarios	H_s (m)	T_p (s)	ϕi (˚)	Wind Speed	
				W_x (m/s)	W_y (m/s)
A#1	3.8	10	270	-20	0
A#2	3.8	4.5	315	-7.07	7.07

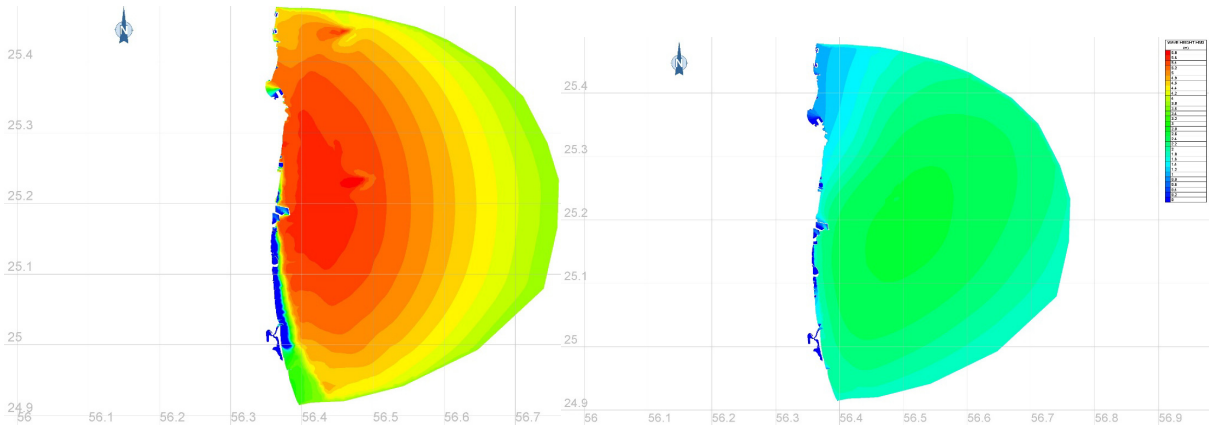

Figure S3.26. Characteristic operational WFS results of H_{mo} (m) by Model A in **Fujairah** (UAE, Persian Gulf; no. 1 of Table 1) port during SE and NE sector rough wave conditions. Scenarios A#1 (left) and A#2 (right).

Scenarios	H_s (m)	T_p (s)	ϕi (˚)	Wind Speed	
				W_x (m/s)	W_y (m/s)
A#1	2.5	6.75	315	-8.49	8.49
A#2	5.5	11	315	-17.68	17.68

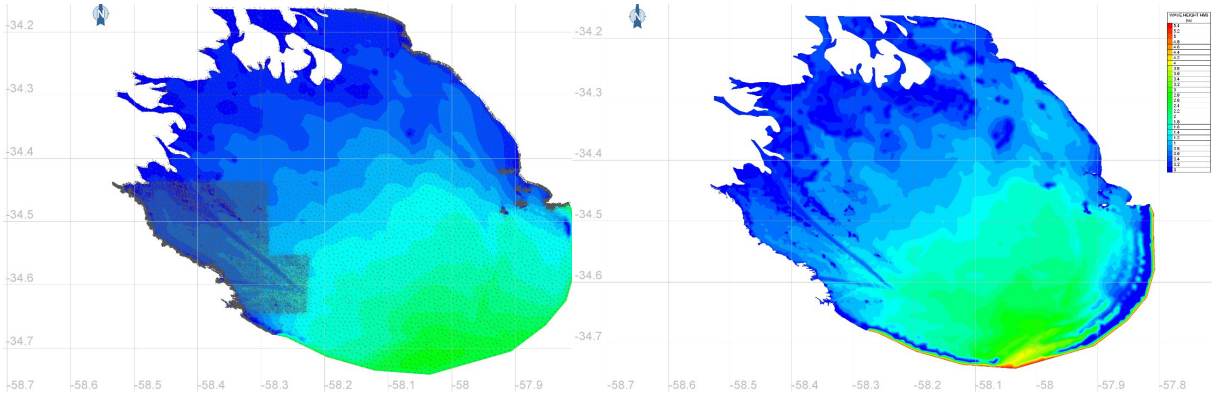

Figure S3.27. Characteristic operational WFS results of H_{mo} (m) by Model A in **Buenos Aires** (Brazil, South Atlantic Ocean; no. 3 of Table 1) port during SE sector moderate and very rough wave conditions. Scenarios A#1 (left) and A#2 (right).

Scenarios	H_s (m)	T_p (s)	ϕi (˚)	Wind Speed	
				W_x (m/s)	W_y (m/s)
A#1	2.5	6.75	335	-5.07	10.88
A#2	5.5	11	335	-10.57	22.66

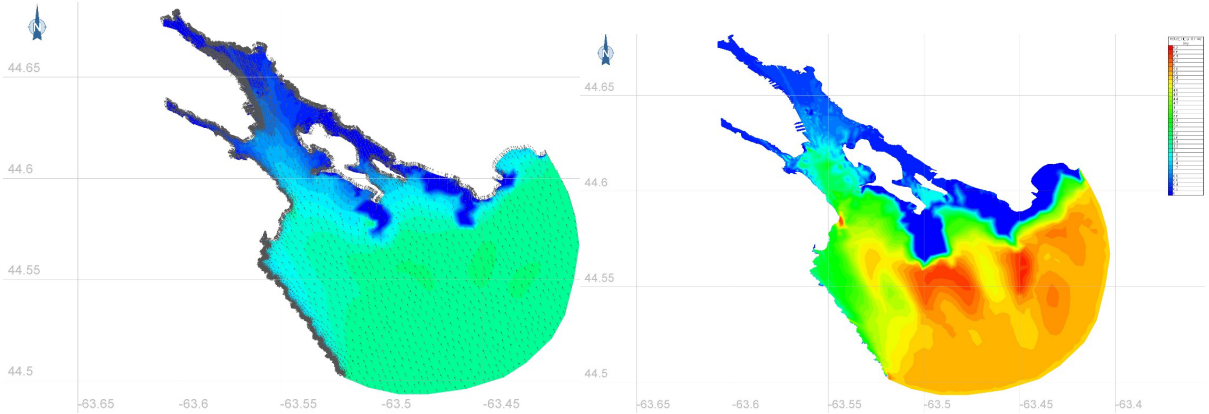

Figure S3.28. Characteristic operational WFS results of H_{mo} (m) by Model A in **Halifax** (Canada, North Atlantic Ocean; no. 8 of Table 1) port during SE sector moderate and very rough wave conditions. Scenarios A#1 (left) and A#2 (right).

Scenarios	H_s (m)	T_p (s)	ϕi (˚)	Wind Speed	
				W_x (m/s)	W_y (m/s)
A#1	3.8	10	135	14.14	-14.14
A#2	1.8	4.5	90	10	0

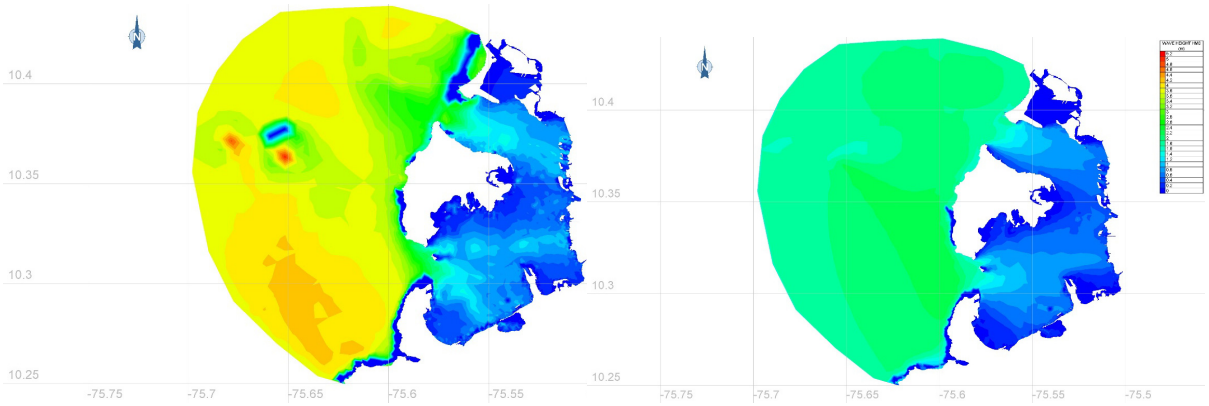

Figure S3.29. Characteristic operational WFS results of H_{mo} (m) by Model A in **Cartagena** (Colombia, Caribbean Sea; no. 9 of Table 1) port during SE sector rough and moderate wave conditions. Scenarios A#1 (left) and A#2 (right).

Scenarios	H_s (m)	T_p (s)	ϕi (˚)	Wind Speed	
				W_x (m/s)	W_y (m/s)
A#1	1.8	4.5	315	-7.07	7.07
A#2	3.8	10.0	315	-14.14	14.14

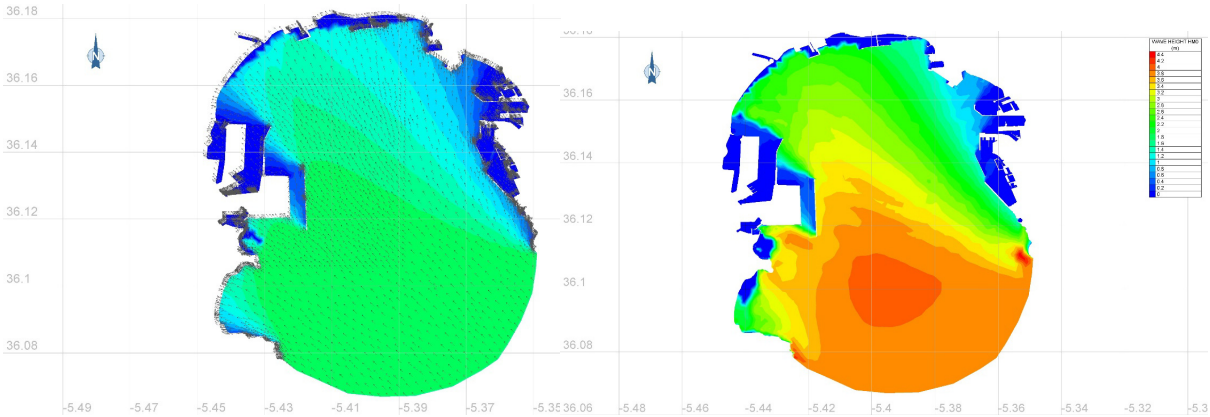

Figure S3.30. Characteristic operational WFS results of H_{mo} (m) by Model A in **Algeciras** (Spain, West Mediterranean Sea; no. 12 of Table 1) port during SE sector moderate and rough wave conditions. Scenarios A#1 (left) and A#2 (right).

Scenarios	H_s (m)	T_p (s)	ϕi (˚)	Wind Speed	SWL (m)

				W_x (m/s)	W_y (m/s)	
A#1	1.8	4.5	135	7.07	-7.07	0.0
A#4	3.8	10	135	14.14	-14.14	+6.0

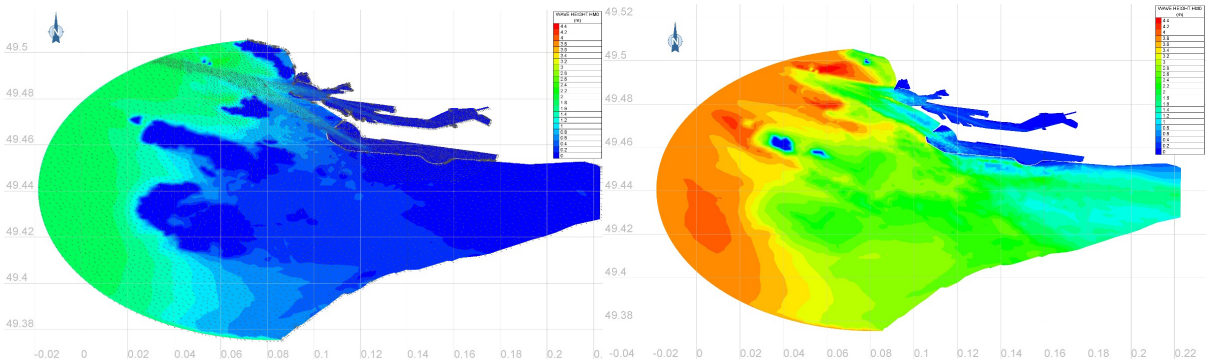

Figure S3.31. Characteristic operational WFS results of H_{mo} (m) by Model A in **Le Havre** (France, East Atlantic Ocean; no. 14 of Table 1) port during NW sector moderate and rough wave conditions. Scenarios A#1 (left) and A#2 (right).

Scenarios	H_s (m)	T_p (s)	ϕi (°)	**Wind Speed**	
				W_x (m/s)	W_y (m/s)
A#1	3.8	10	90	20	0
A#2	1.8	4.5	180	0	-10

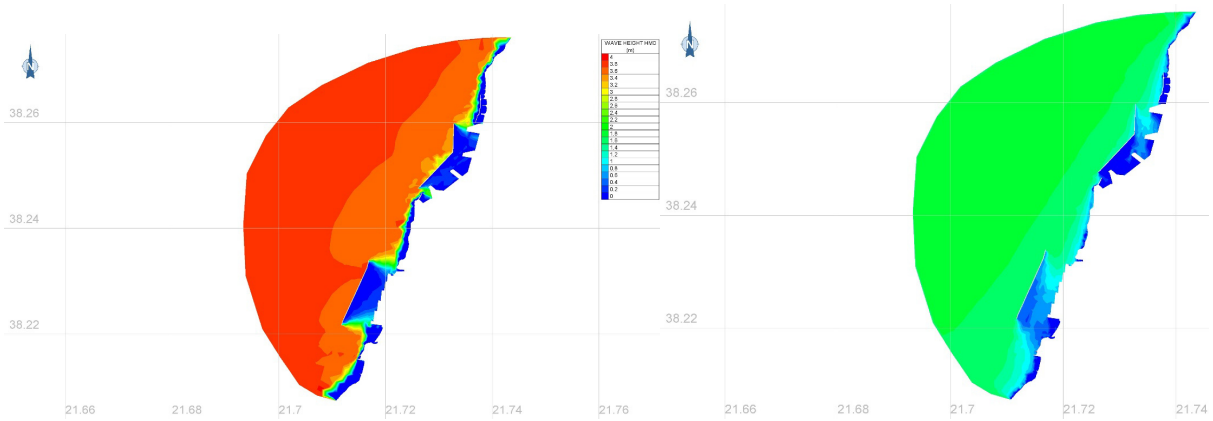

Figure S3.32. Characteristic operational WFS results of H_{mo} (m) by Model A in **Patra** (Greece, East-central Mediterranean Sea; no. 16 of Table 1) port during NW sector rough and moderate wave conditions. Scenarios A#1 (left) and A#2 (right).

Scenarios	H_s (m)	T_p (s)	ϕi (°)	**Wind Speed**	
				W_x (m/s)	W_y (m/s)

A#1	3.8	10	0	0	20
A#2	1.8	4.5	315	-7.07	7.07

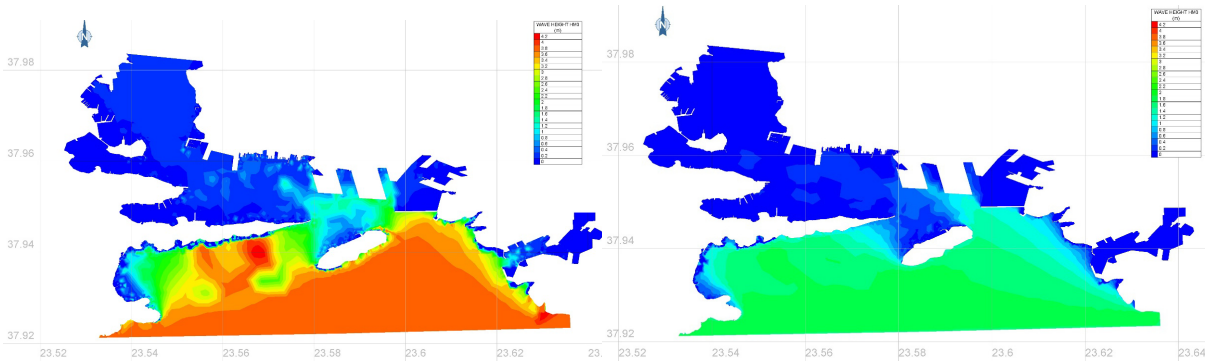

Figure S3.33. Characteristic operational WFS results of H_{mo} (m) by Model A in **Piraeus** (Greece, West-central Aegean Sea; no. 17 of Table 1) port during S and SE sector rough and moderate wave conditions. Scenarios A#1 (left) and A#2 (right).

Scenarios	**H_s (m)**	**T_p (s)**	**ϕi (˚)**	**Wind Speed**	
				W_x (m/s)	**W_y (m/s)**
A#1	3.8	10.0	45	10.6	10.6
A#2	3.8	10.0	0	0.0	15.0

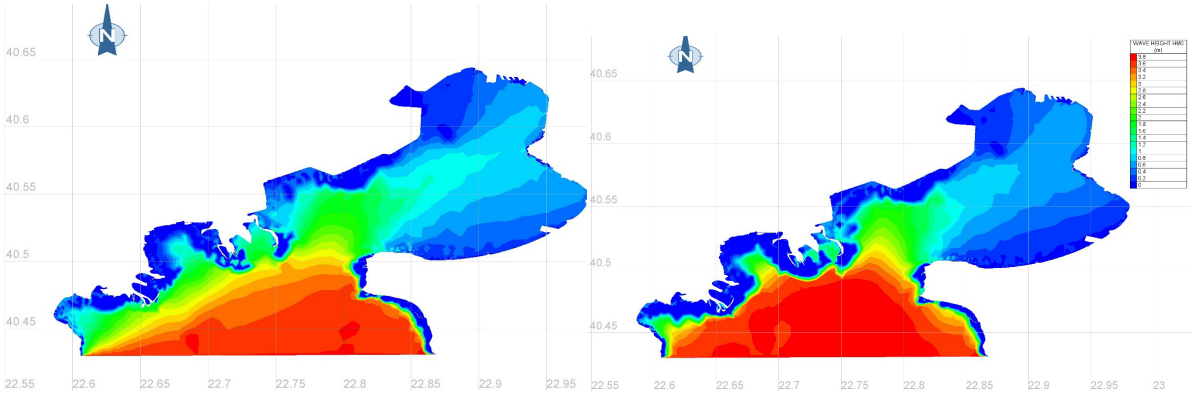

Figure S3.34. Characteristic operational WFS results of H_{mo} (m) by Model A in **Thessaloniki** (Greece, North-western Aegean Sea; no. 18 of Table 1) port during SW and S sector rough wave conditions. Scenarios A#1 (left) and A#2 (right).

Scenarios	**H_s (m)**	**T_p (s)**	**ϕi (˚)**	**Wind Speed**	
				W_x (m/s)	**W_y (m/s)**
A#1	1.8	4.5	270	-10.0	0.0

A#2	3.8	10.0	315	-10.6	10.6

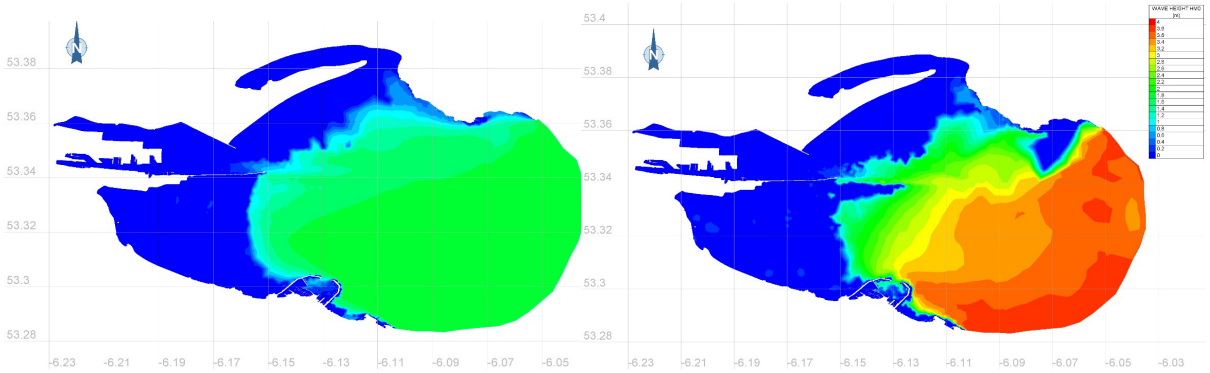

Figure S3.35. Characteristic operational WFS results of H_{mo} (m) by Model A in **Dublin** (Ireland, North Sea; no. 21 of Table 1) port during E and SE sector moderate and rough wave conditions. Scenarios A#1 (left) and A#2 (right).

Scenarios	**H_s (m)**	**T_p (s)**	**ϕi (˚)**	**Wind Speed**	
				W_x (m/s)	**W_y (m/s)**
A#1	3.8	10	180	0	-20
A#2	1.8	4.5	135	7.07	7.07

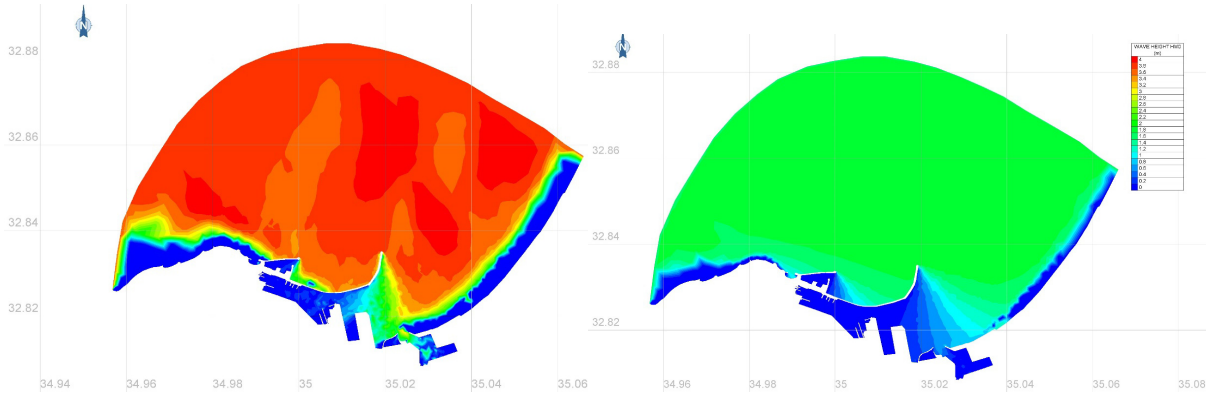

Figure S3.36. Characteristic operational WFS results of H_{mo} (m) by Model A in **Haifa** (Israel, East Mediterranean Sea; no. 22 of Table 1) port during N and NW sector rough and moderate wave conditions. Scenarios A#1 (left) and A#2 (right).

Scenarios	**H_s (m)**	**T_p (s)**	**ϕi (˚)**	**Wind Speed**	
				W_x (m/s)	**W_y (m/s)**
A#1	2.5	6.75	50	11.49	9.64
A#2	2.5	6.75	290	-11.27	4.10

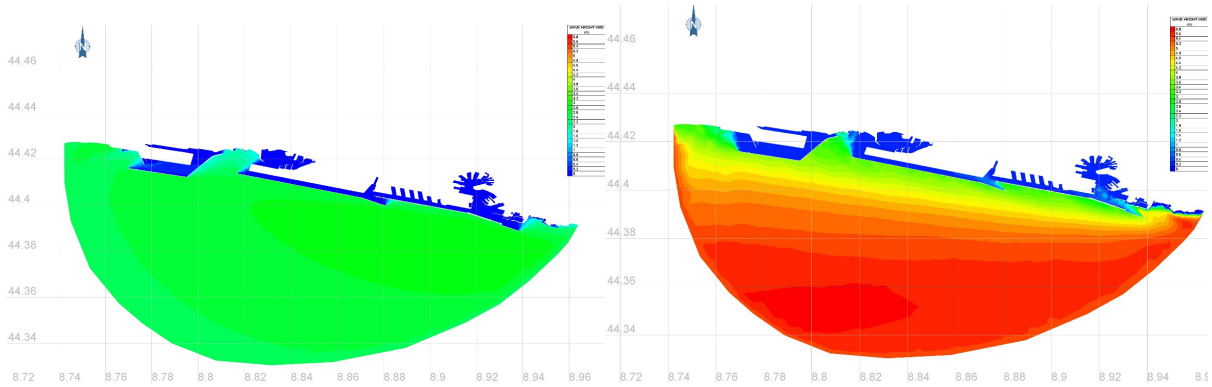

Figure S3.37. Characteristic operational WFS results of H_{mo} (m) by Model A in **Genova** (Italy, North Mediterranean Sea; no. 25 of Table 1) port during SW and E-SE sector moderate wave conditions. Scenarios A#1 (left) and A#2 (right).

Scenarios	H_s (m)	T_p (s)	ϕi (˚)	Wind Speed	
				W_x (m/s)	W_y (m/s)
A#1	1.8	4.5	340	-3.42	9.40
A#2	3.8	10	340	-6.84	18.79

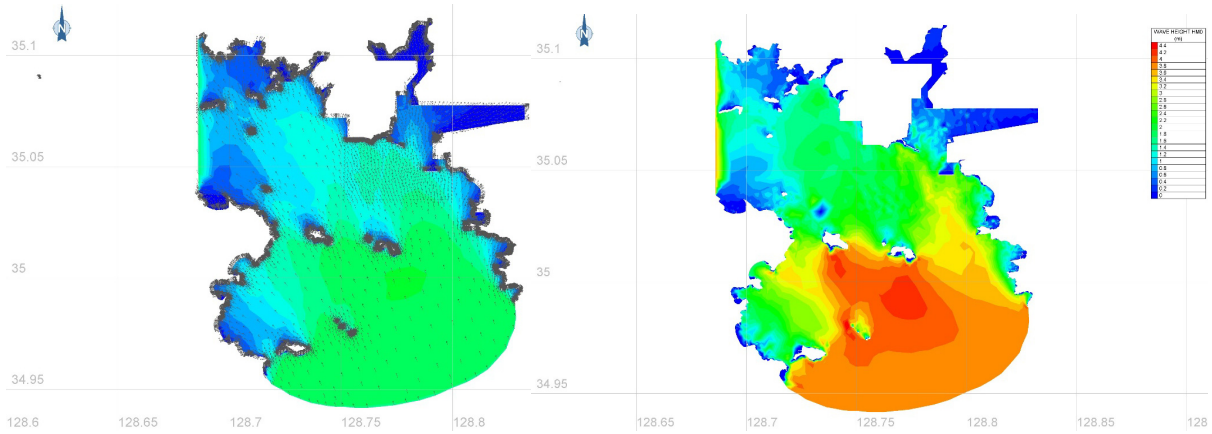

Figure S3.38. Characteristic operational WFS results of H_{mo} (m) by Model A in **Busan** (South Korea, Yellow Sea; no. 29 of Table 1) port during S-SE sector moderate and rough wave conditions. Scenarios A#1 (left) and A#2 (right).

Scenarios	H_s (m)	T_p (s)	ϕi (˚)	Wind Speed	
				W_x (m/s)	W_y (m/s)
A#1	5.5	11	90	25	0
A#2	3.8	10	150	10	-17.32

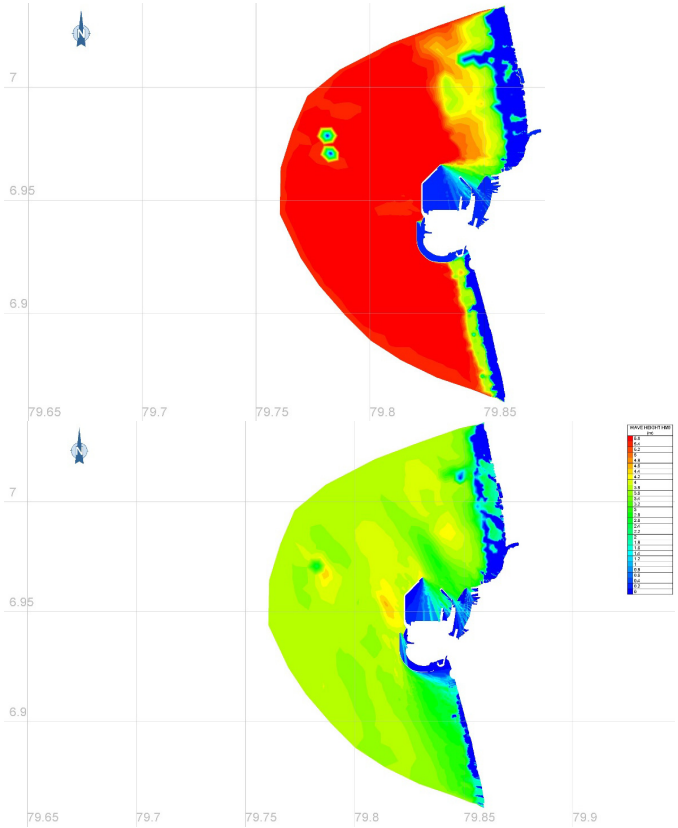

Figure S3.39. Characteristic operational WFP results of H_{mo} (m) by Model A in **Colombo** (Sri Lanka, Laccadive Sea; no. 31 of Table 1) port during W and NW sector very rough and moderate wave conditions. Scenarios A#1 (left) and A#2 (right).

Scenarios	H_s (m)	T_p (s)	ϕi (˚)	Wind Speed	
				W_x (m/s)	W_y (m/s)
A#1	2.5	6.75	235	-9.83	-6.88
A#2	5.5	11.0	90	25.0	0.0

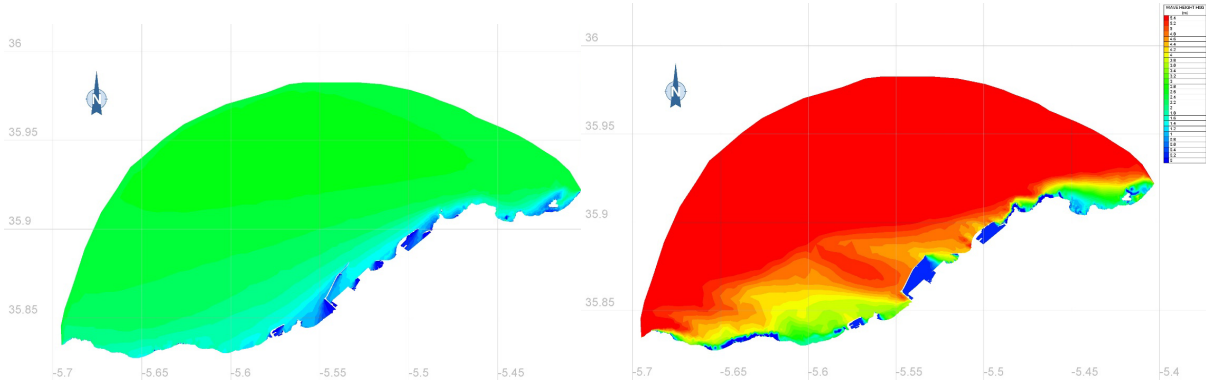

Figure S3.40. Characteristic operational WFP results of H_{mo} (m) by Model A in **Tanger Med** (Morocco, West Mediterranean Sea; no. 32 of Table 1) port during NE and W sector moderate and very rough wave conditions. Scenarios A#1 (left) and A#2 (right).

Scenarios	H_s (m)	T_p (s)	ϕi (˚)	Wind Speed	
				W_x (m/s)	W_y (m/s)
A#1	1.8	4.5	135	7.07	-7.07
A#2	3.8	10.0	135	14.14	-14.14

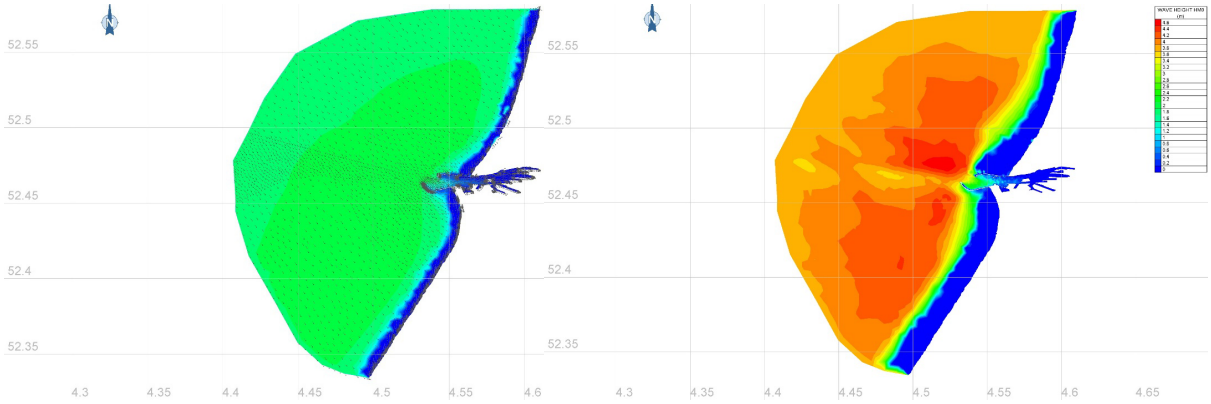

Figure S3.41. Characteristic operational WFP results of H_{mo} (m) by Model A in **IJmuiden** (Netherlands, North Sea; no. 35 of Table 1) port during NW sector moderate and rough wave conditions. Scenarios A#1 (left) and A#2 (right).

Scenarios	H_s (m)	T_p (s)	ϕi (˚)	Wind Speed	
				W_x (m/s)	W_y (m/s)
A#1	2.5	6.75	90	15	0
A#2	5.5	11	90	25	0

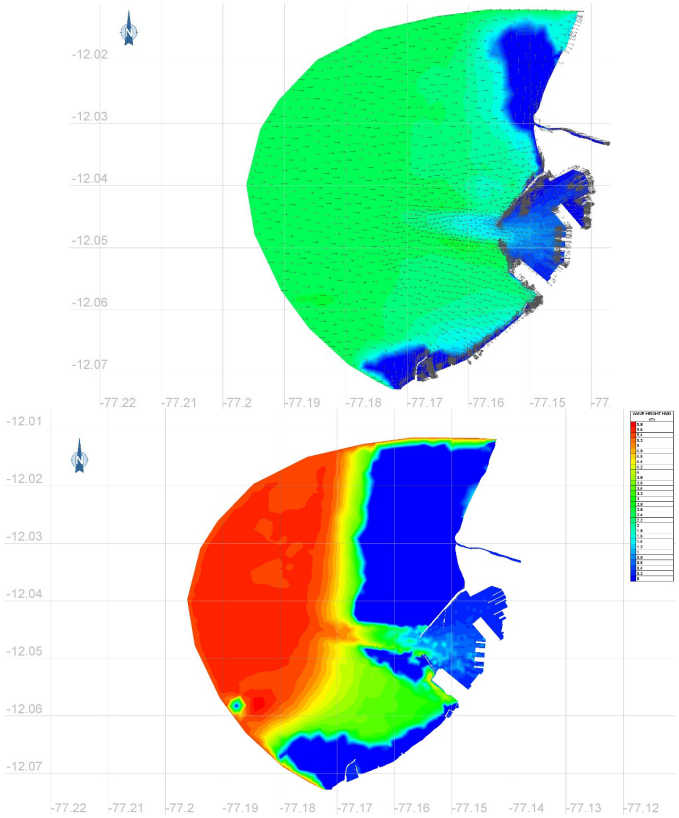

Figure S3.42. Characteristic operational WFP results of H_{mo} (m) by Model A in **Callao** (Peru, South Pacific Ocean; no. 37 of Table 1) port during W sector moderate and very rough wind wave and swell conditions. Scenarios A#1 (left) and A#2 (right).

Scenarios	H_s (m)	T_p (s)	ϕi (˚)	Wind Speed	
				W_x (m/s)	W_y (m/s)
A#1	2.5	6.75	0	0	12
A#2	5.5	11	315	-17.68	17.68

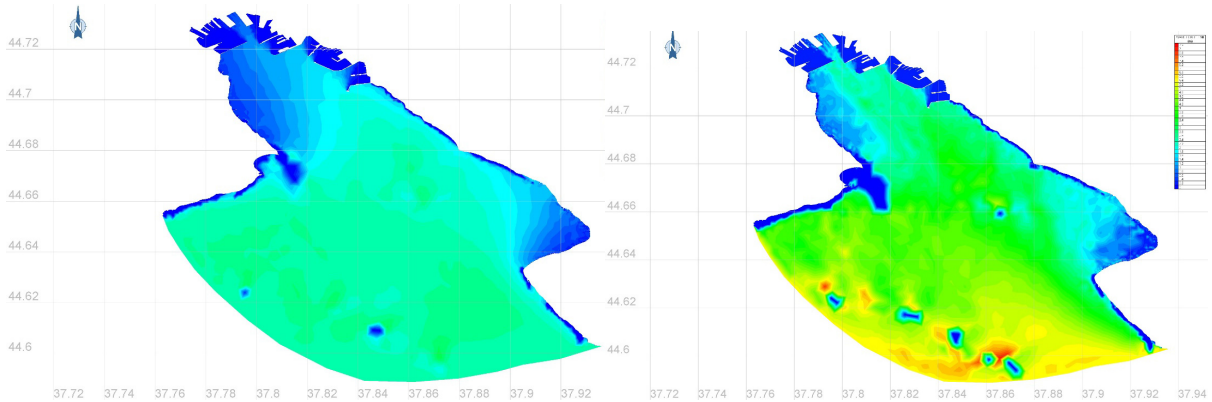

Figure S3.43. Characteristic operational WFP results of H_{mo} (m) by Model A in **Novorossiysk** (Russia, Black Sea; no. 40 of Table 1) port during S and SE sector moderate and very rough wind wave and swell conditions. Scenarios A#1 (left) and A#2 (right).

Scenarios	H_s (m)	T_p (s)	ϕi (˚)	Wind Speed	
				W_x (m/s)	W_y (m/s)
A#1	3.8	10	45	14.14	14.14
A#2	1.8	4.5	90	10	0

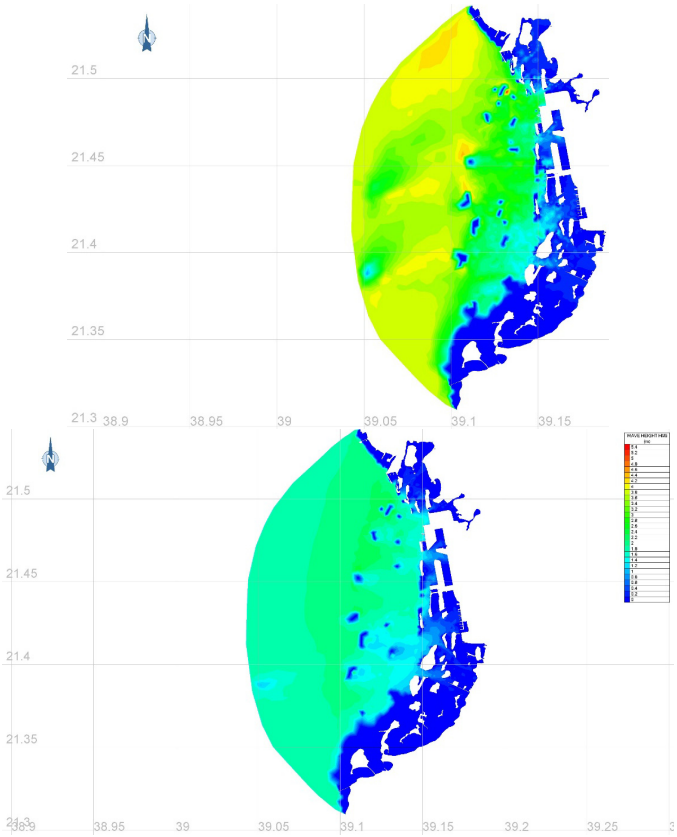

Figure S3.44. Characteristic operational WFP results of H_{mo} (m) by Model A in **Jeddah** (Saudi Arabia, Red Sea; no. 41 of Table 1) port during SW and W sector rough and moderate wind wave and swell conditions. Scenarios A#1 (left) and A#2 (right).

Scenarios	H_s (m)	T_p (s)	ϕi (˚)	Wind Speed	
				W_x (m/s)	W_y (m/s)
A#1	3.8	10.0	315	-14.14	14.14
A#2	1.8	4.5	0	0.0	10.0

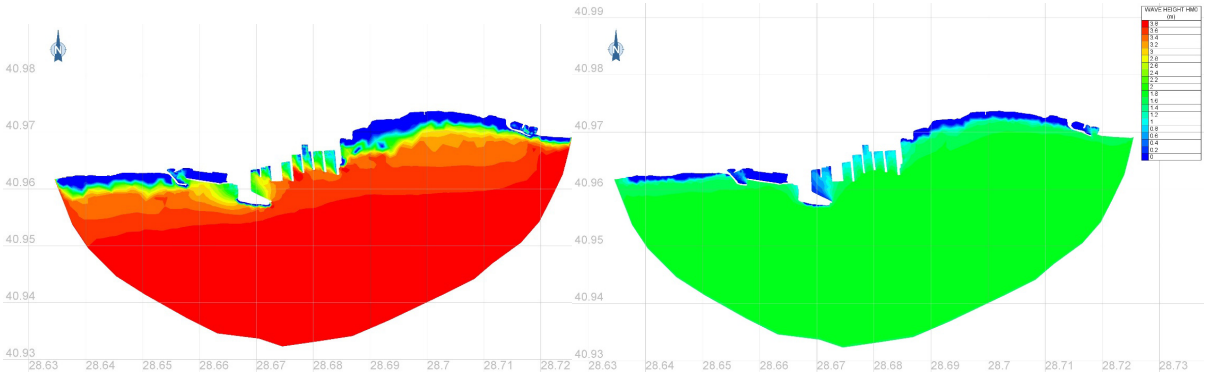

Figure S3.45. Characteristic operational WFP results of H_{mo} (m) by Model A in **Ambarli** (Turkey, Sea of Marmara; no. 44 of Table 1) port during SE and S sector rough and moderate wind wave and swell conditions. Scenarios A#1 (left) and A#2 (right).

Scenarios	H_s (m)	T_p (s)	ϕi (˚)	Wind Speed	
				W_x (m/s)	W_y (m/s)
A#1	2.80	6.75	180	0	-13
A#2	2.80	6.75	225	-9.19	-9.19

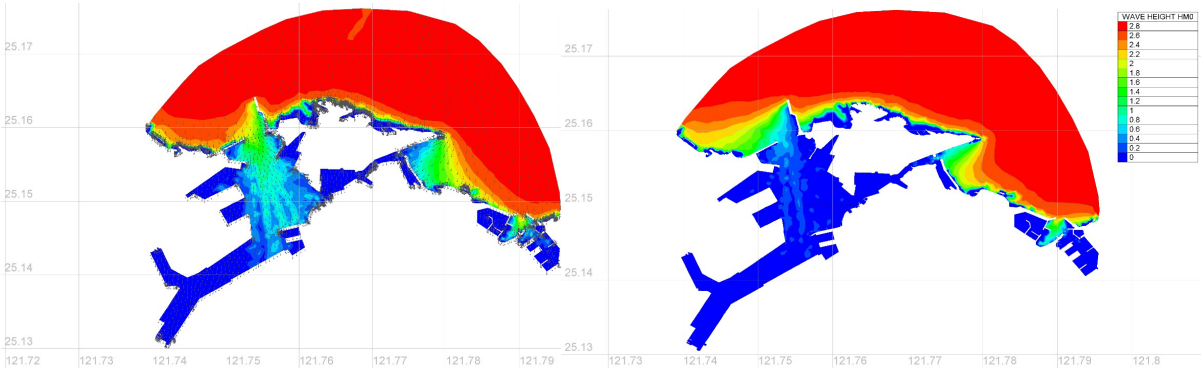

Figure S3.46. Characteristic operational WFP results of H_{mo} (m) by Model A in **Keelung** (Taiwan, East China Sea; no. 45 of Table 1) port during N and NW sector moderate wind wave and swell conditions. Scenarios A#1 (left) and A#2 (right).

Supplementary Material S4

Figures of characteristic results by simulations with Model B in 22 of the aforesaid 49 ports are provided. All simulations refer to typical (unity for height) wave conditions and highly detailed depictions of the wave-induced agitation inside and around the entrance of the harbour basins (Model B).

Scenarios	H_s (m)	T_p (s)	ϕi (°)	t_{sim} (s)
B#1 (2.1)	1.00	8.00	270	1200
B#2 (2.2)	1.00	8.00	315	1200
B#3 (2.3)	1.00	8.00	225	1200

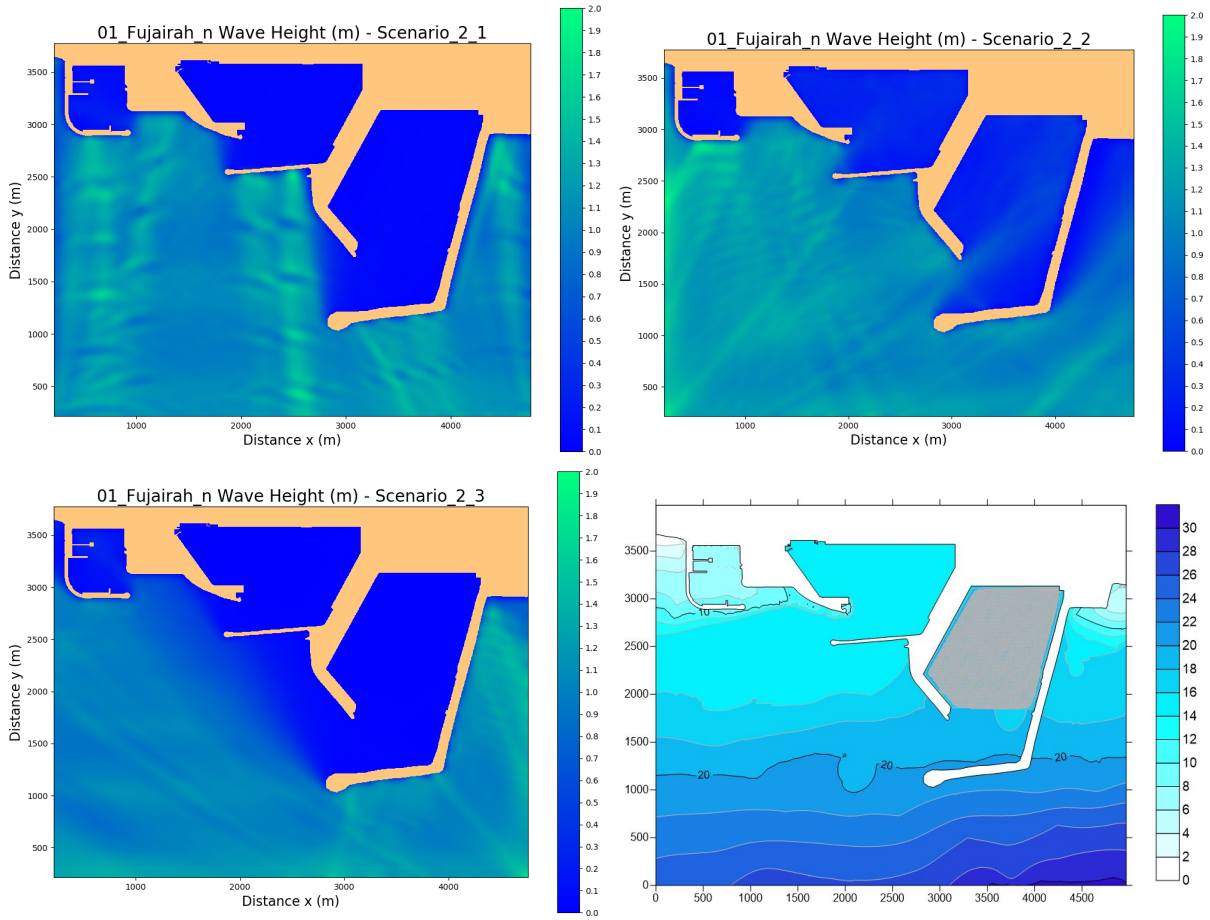

Figure S4.1. Characteristic operational WFS results of Hs (m) by Model B in **Fujairah** (UAE; no. 1 of Table 1) port during E, SE, and NE sector incoming waves of H_s=1m (port orientation is turned 90° clockwise).

Scenarios	H_s (m)	T_p (s)	ϕi (°)	t_{sim} (s)
B#1 (3.1)	1.00	12.0	270	1000
B#2 (3.2)	1.00	12.0	315	1000
B#3 (3.3)	1.00	12.0	225	1000

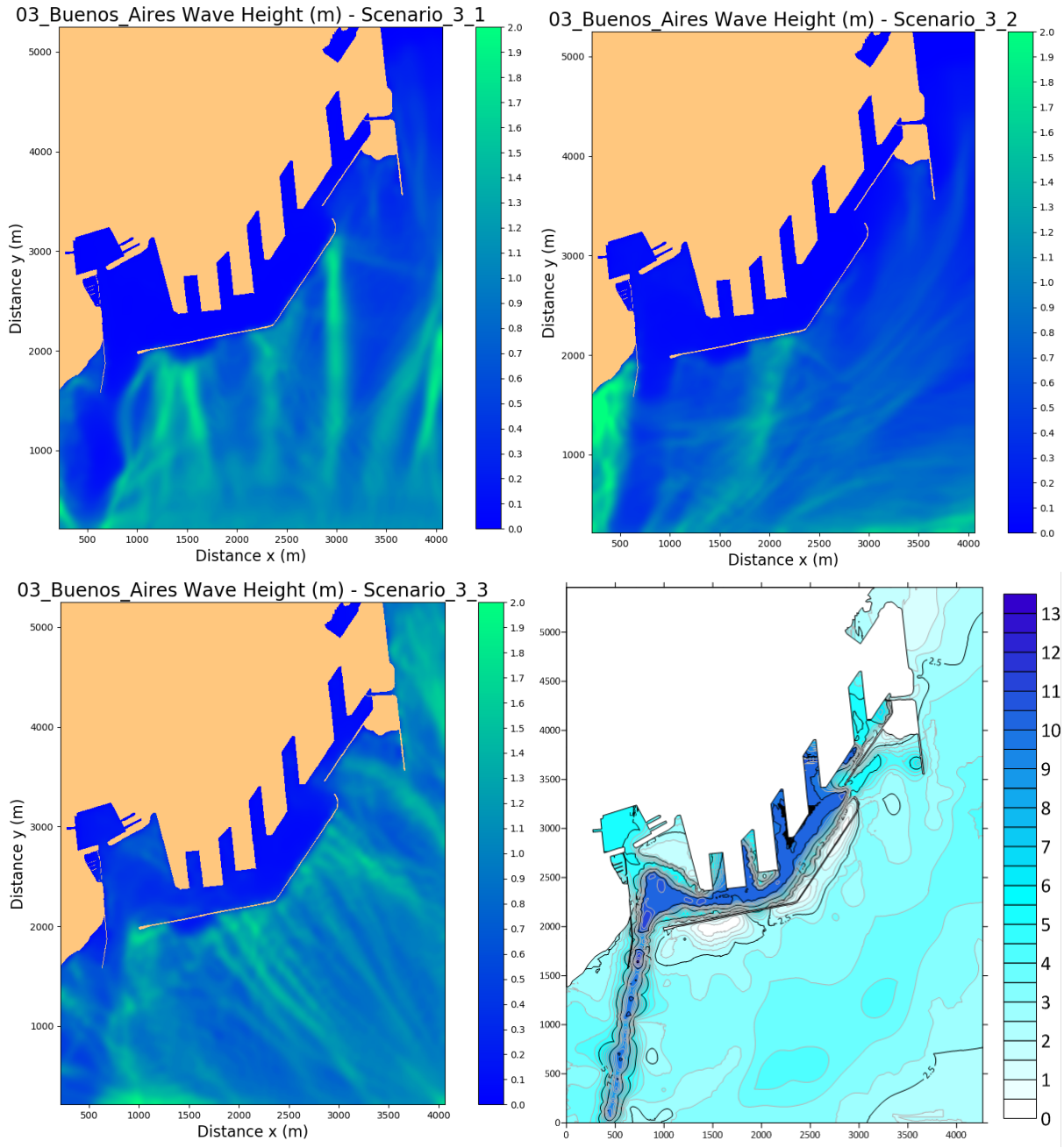

Figure S4.2. Characteristic operational WFS results of Hs (m) by Model B in **Buenos Aires** (Brazil; no. 3 of Table 1) port during E, SE, and NE sector incoming waves of H_s=1m (port orientation is turned 90° clockwise).

Scenarios	H_s (m)	T_p (s)	ϕi (˚)	t_{sim} (s)
B#1 (2.1)	1.00	8.00	270	800
B#2 (2.2)	1.00	8.00	315	800
B#3 (2.3)	1.00	8.00	0	800

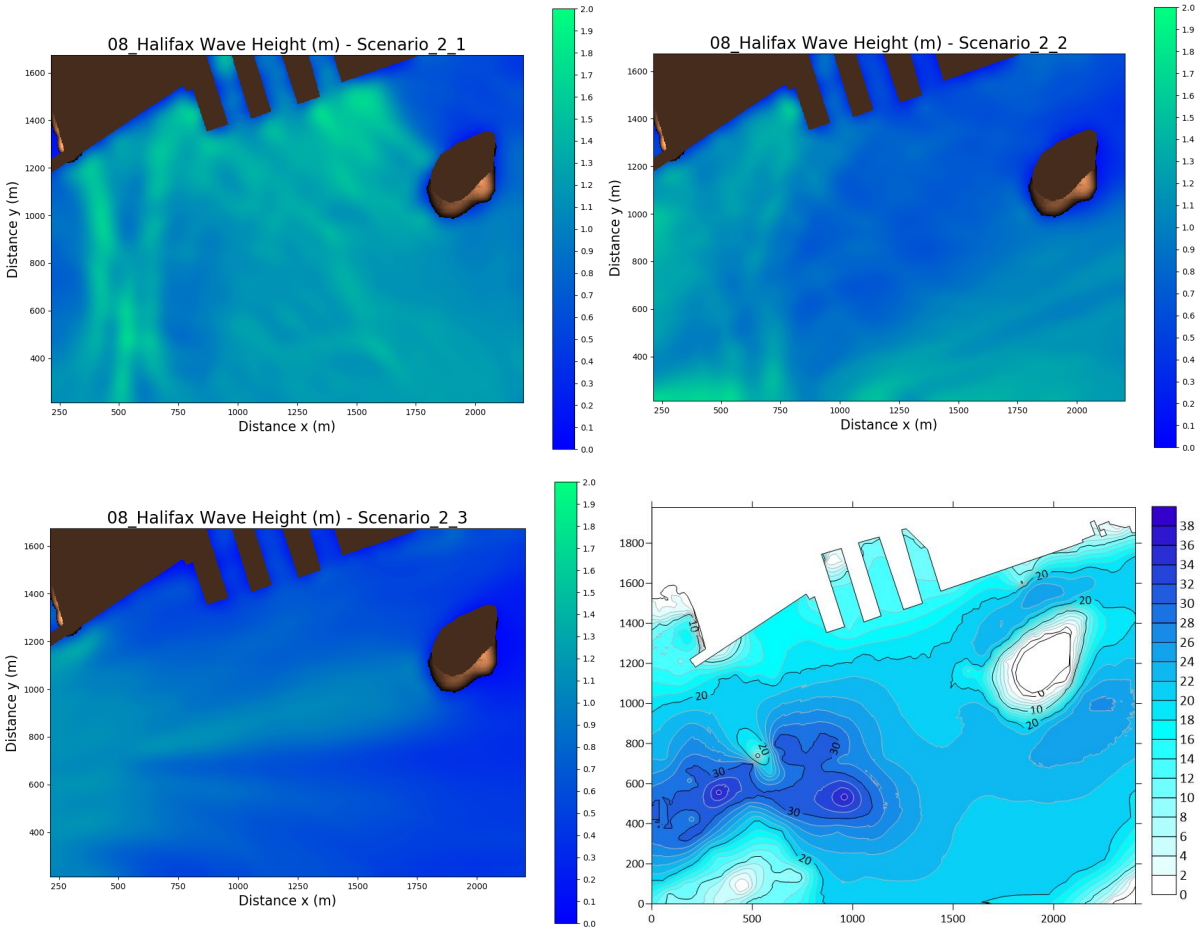

Figure S4.3. Characteristic operational WFS results of Hs (m) by Model B in **Halifax** (Canada; no. 8 of Table 1) port during E, SE, and S sector incoming waves of H_s=1m (port orientation is turned 90° clockwise).

Scenarios	H_s (m)	T_p (s)	ϕi (˚)	t_{sim} (s)

B#1 (3.1)	1.00	12.0	90	1300
B#2 (3.2)	1.00	12.0	135	1300
B#3 (3.3)	1.00	12.0	45	1300

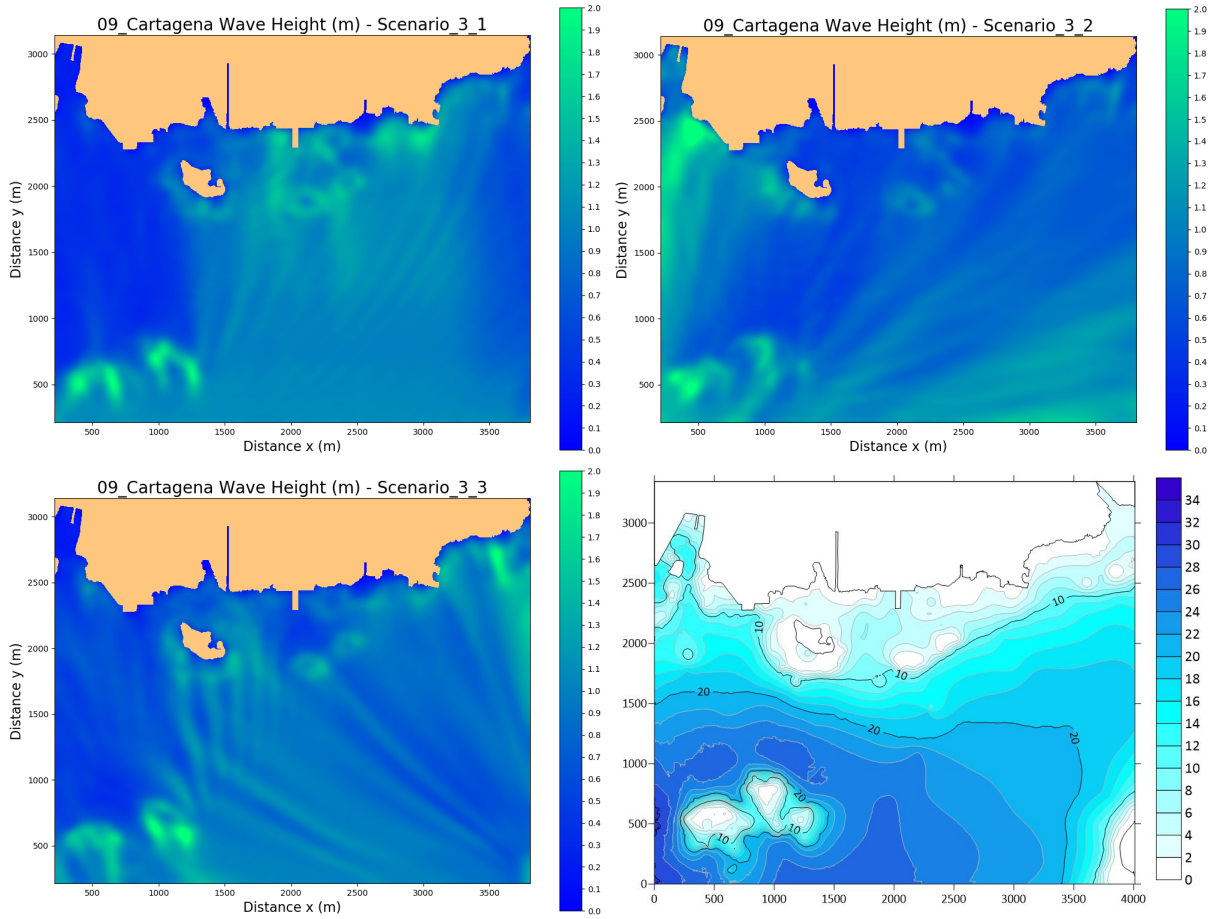

Figure S4.4. Characteristic operational WFS results of Hs (m) by Model B in **Cartagena** (Colombia; no. 9 of Table 1) port during W, NW, and SW sector incoming waves of H_s=1m (port orientation is turned 90° counter-clockwise).

Scenarios	**H_s (m)**	**T_p (s)**	**ϕi (˚)**	**t_{sim} (s)**
B#1 (2.1)	1.00	8.00	270	1200

B#2 (2.2)	1.00	8.00	315	1200
B#3 (2.3)	1.00	8.00	0	1200

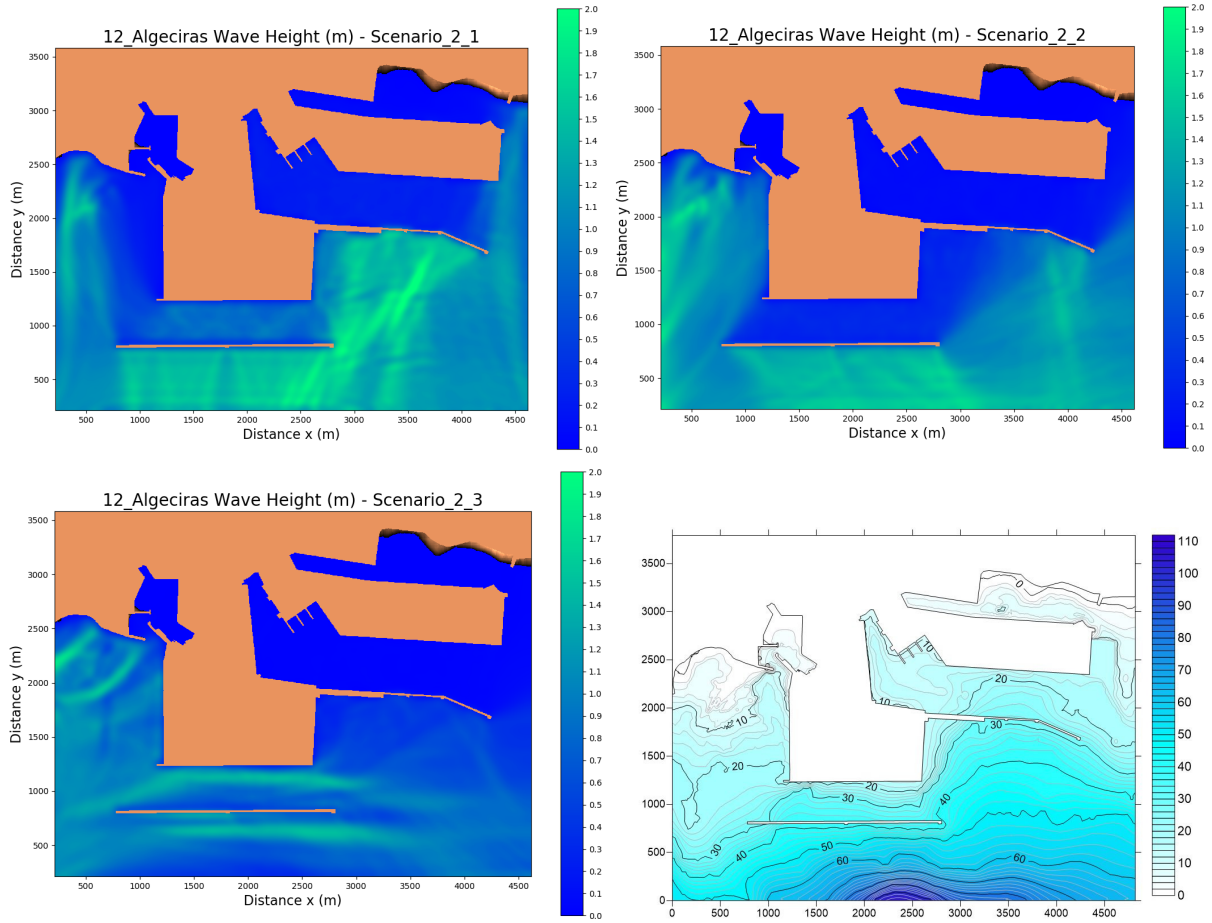

Figure S4.5. Characteristic operational WFS results of Hs (m) by Model B in **Algeciras** (Spain; no. 12 of Table 1) port during E, SE, and S sector incoming waves of H_s=1m (port orientation is turned 90° clockwise).

Scenarios	**H_s (m)**	**T_p (s)**	**ϕi (˚)**	**t_{sim} (s)**
B#1 (3.1)	1.00	12.0	90	1200
B#2 (3.2)	1.00	12.0	135	1200
B#3 (3.3)	1.00	12.0	45	1200

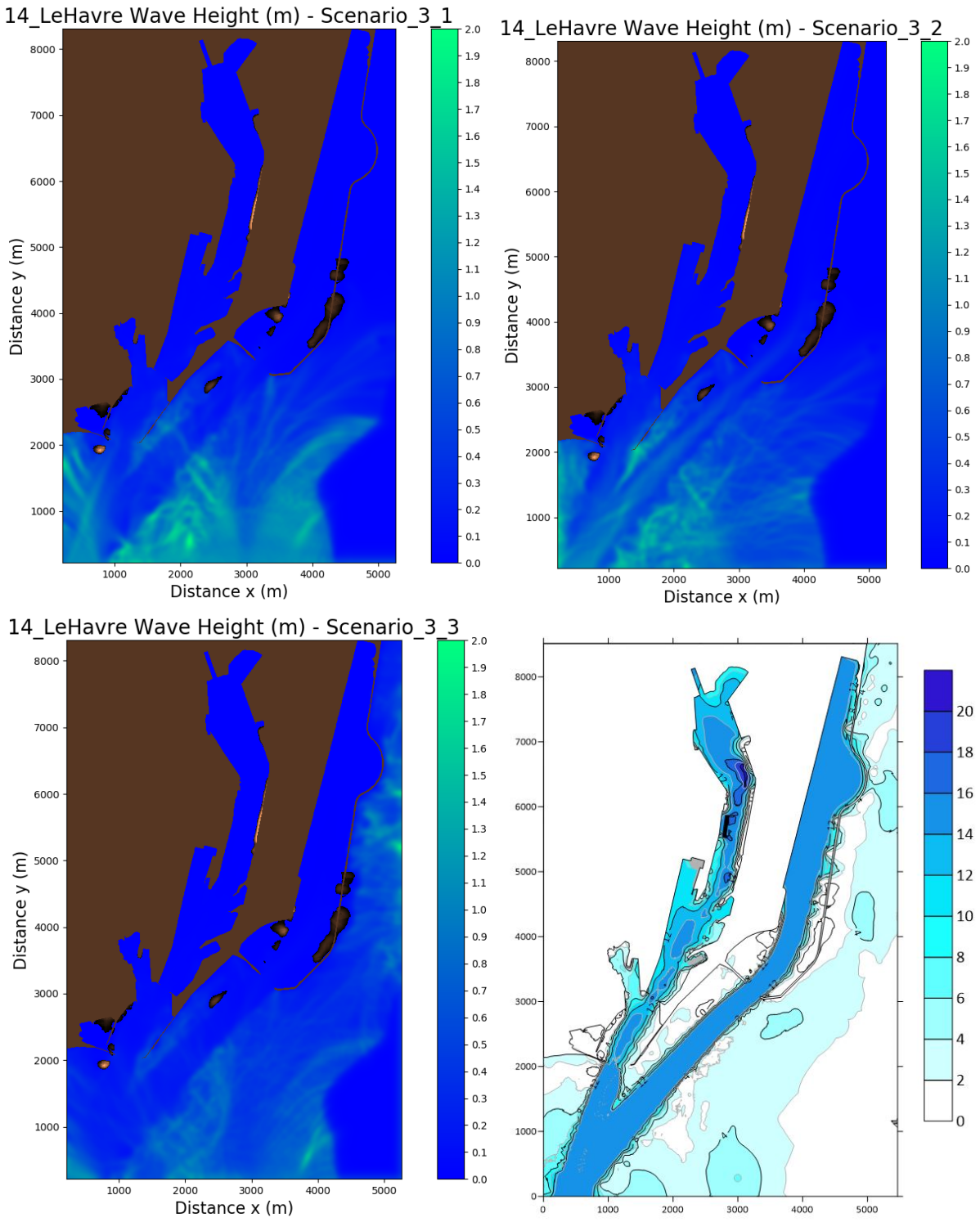

Figure S4.6. Characteristic operational WFS results of Hs (m) by Model B in **Le Havre** (France; no. 14 of Table 1) port during W, NW, and SW sector incoming waves of H_s=1m (port orientation 90° counter-clockwise).

Scenarios	**H_s (m)**	**T_p (s)**	**ϕi (˚)**	**t_{sim} (s)**
B#1 (3.1)	1.00	12.0	90	500
B#2 (3.2)	1.00	12.0	135	500
B#3 (3.3)	1.00	12.0	45	500

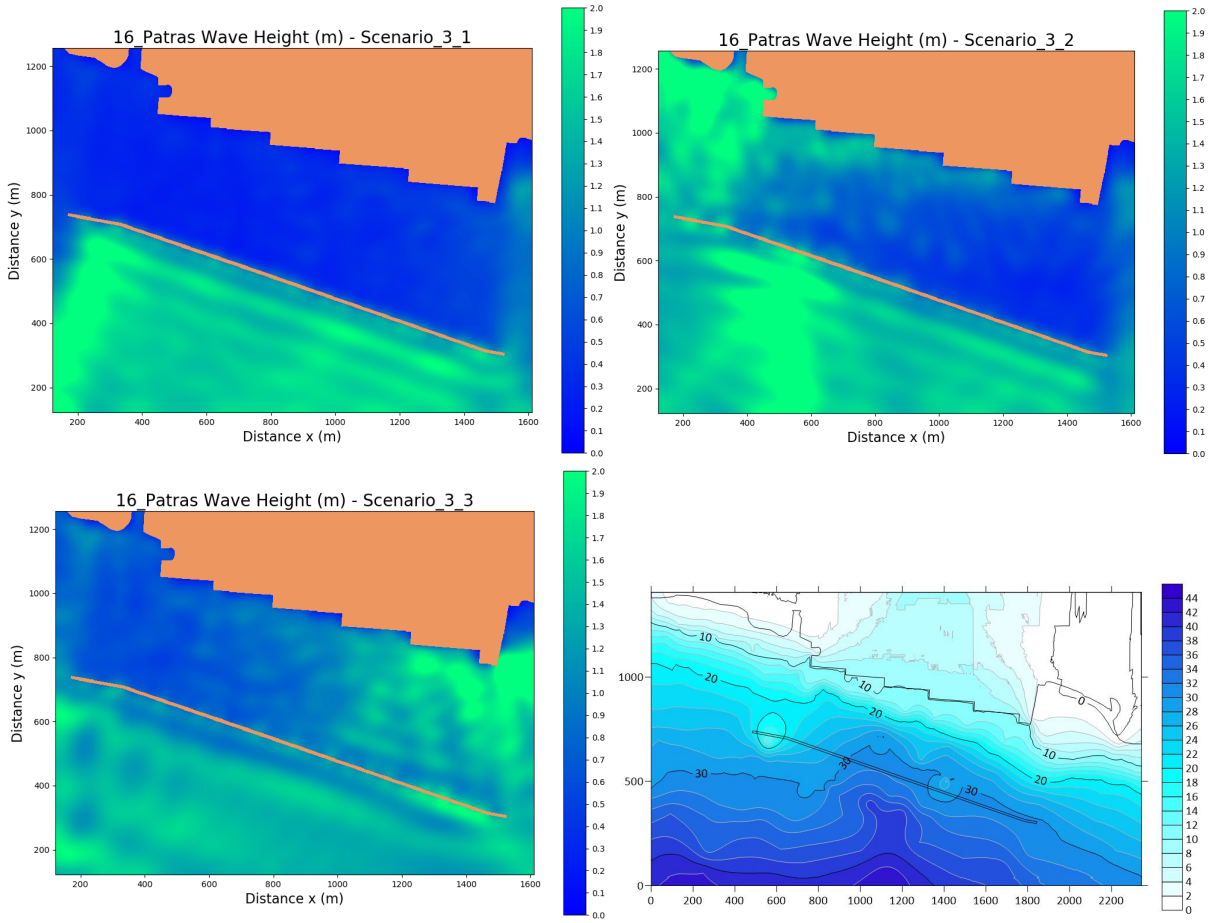

Figure S4.7. Characteristic operational WFS results of Hs (m) by Model B in **Patra** (Greece; no. 16 of Table 1) port during W, NW, and SW sector incoming waves of H_s=1m (port orientation is turned 90° counter-clockwise).

Scenarios	**H_s (m)**	**T_p (s)**	**ϕi (°)**	**t_{sim} (s)**
B#1 (2.1)	1.00	8.00	0	1000
B#2 (2.2)	1.00	8.00	45	1000
B#3 (2.3)	1.00	8.00	315	1000

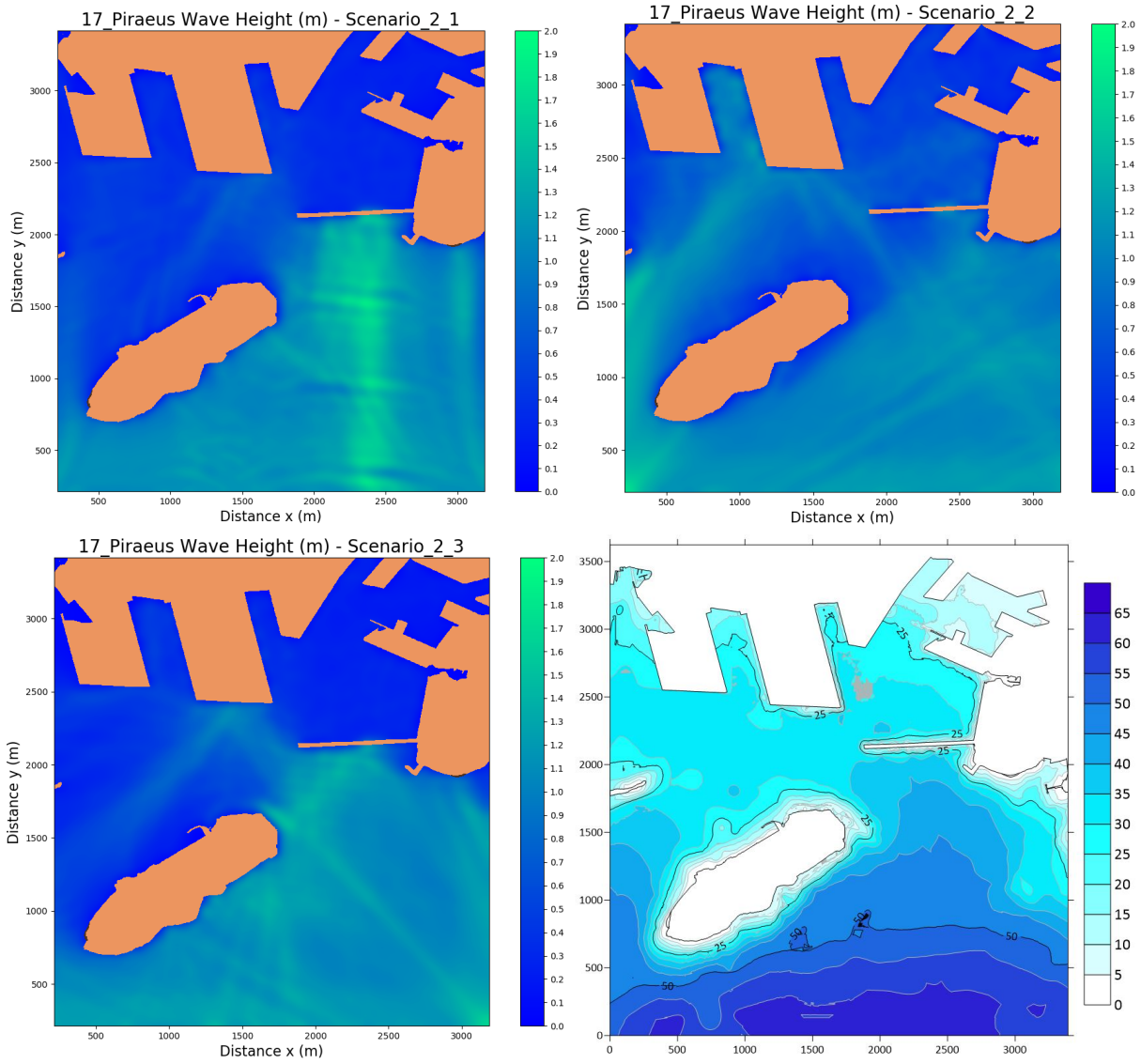

Figure S4.8. Characteristic operational WFS results of Hs (m) by Model B in **Piraeus** (Greece; no. 17 of Table 1) port during S, SW, and SE sector incoming waves of H_s=1m.

Scenarios	**H_s (m)**	**T_p (s)**	**ϕi (˚)**	**t_{sim} (s)**
B#1 (2.1)	1.00	8.00	0	700
B#2 (2.2)	1.00	8.00	45	700
B#3 (2.3)	1.00	8.00	315	700

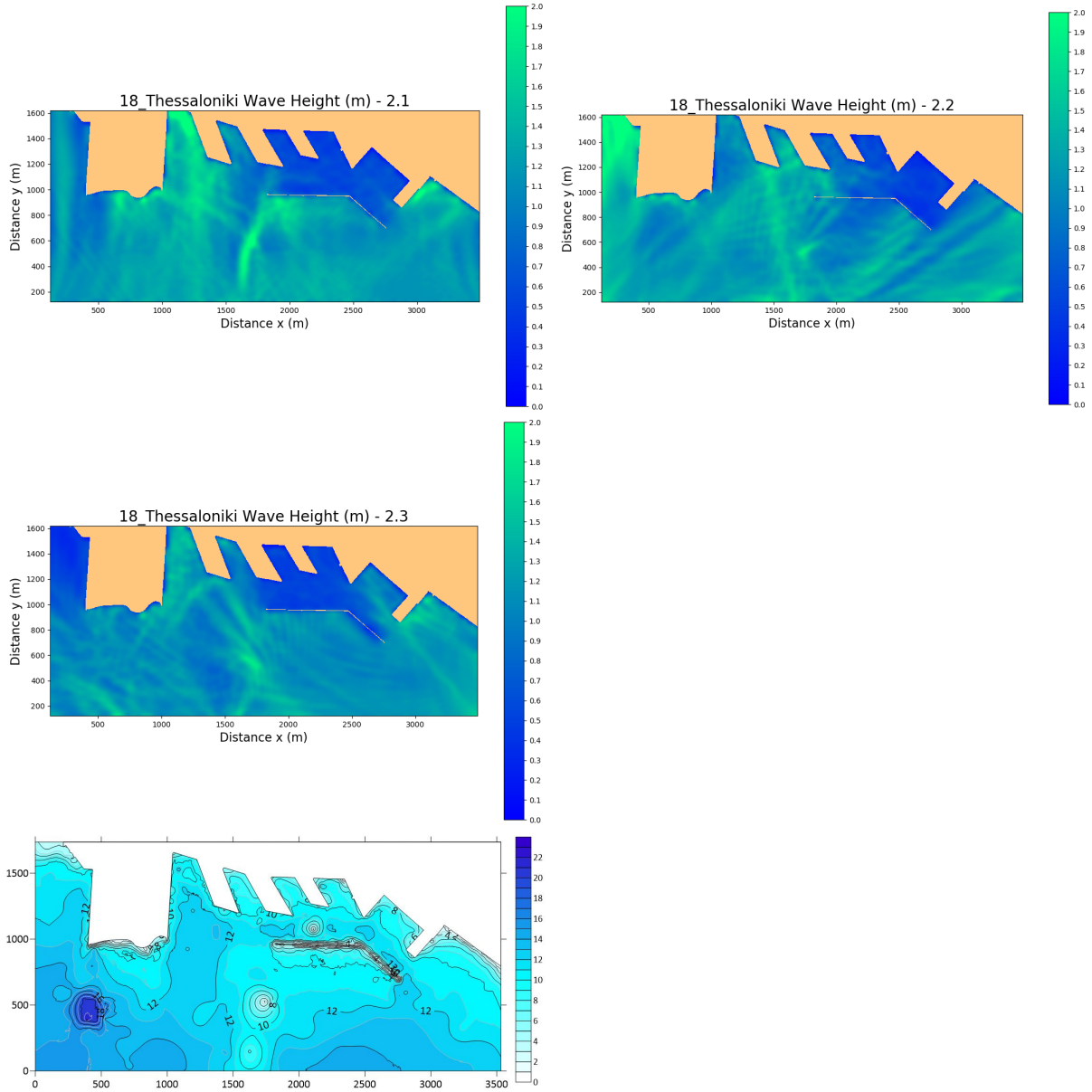

Figure S4.9. Characteristic operational WFS results of Hs (m) by Model B in **Thessaloniki** (Greece; no. 18 of Table 1) port during S, SW, and SE sector incoming waves of H_s=1m.

Scenarios	H_s (m)	T_p (s)	ϕi (˚)	t_{sim} (s)
B#1 (2.1)	1.00	8.00	270	1700
B#2 (2.2)	1.00	8.00	315	1700
B#3 (3.1)	1.00	12.0	270	1700

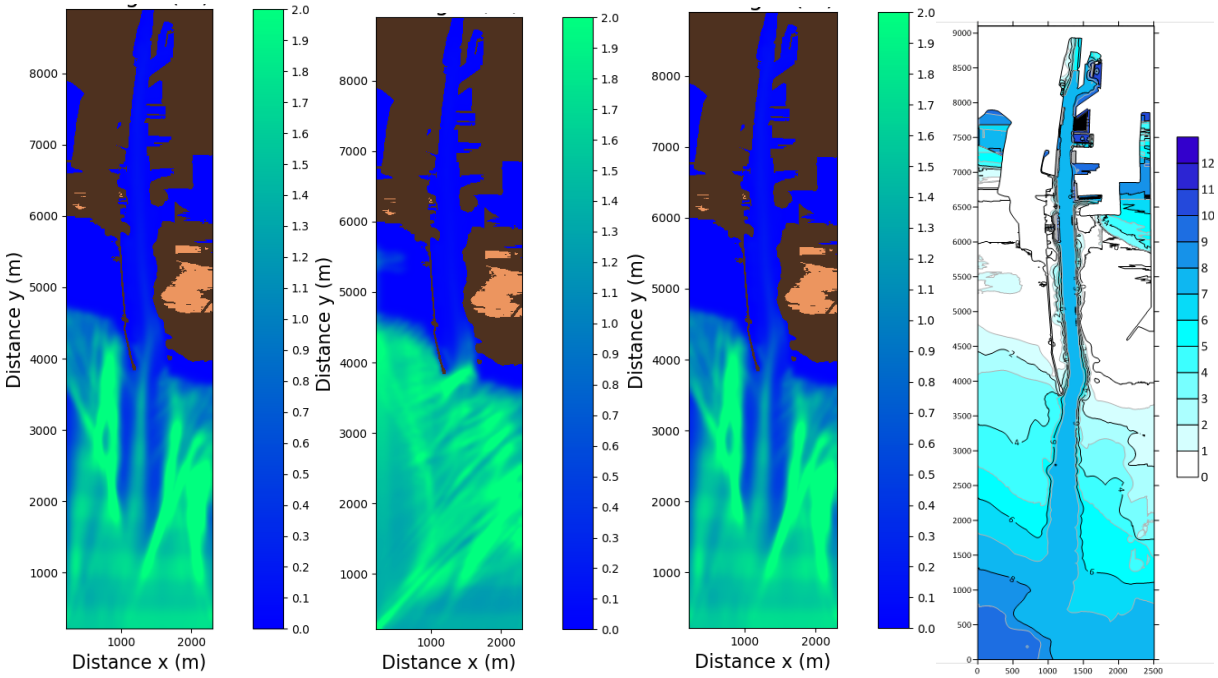

Figure S4.10. Characteristic operational WFS results of Hs (m) by Model B in **Dublin** (Ireland; no. 21 of Table 1) port during E and SE sector incoming wind waves and swell of H_s=1m (port orientation is turned 90° clockwise).

Scenarios	H_s (m)	T_p (s)	ϕi (˚)	t_{sim} (s)

B#1 (2.1)	1.00	8.00	180	1400
B#2 (2.2)	1.00	8.00	225	1400
B#3 (2.3)	1.00	8.00	135	1400

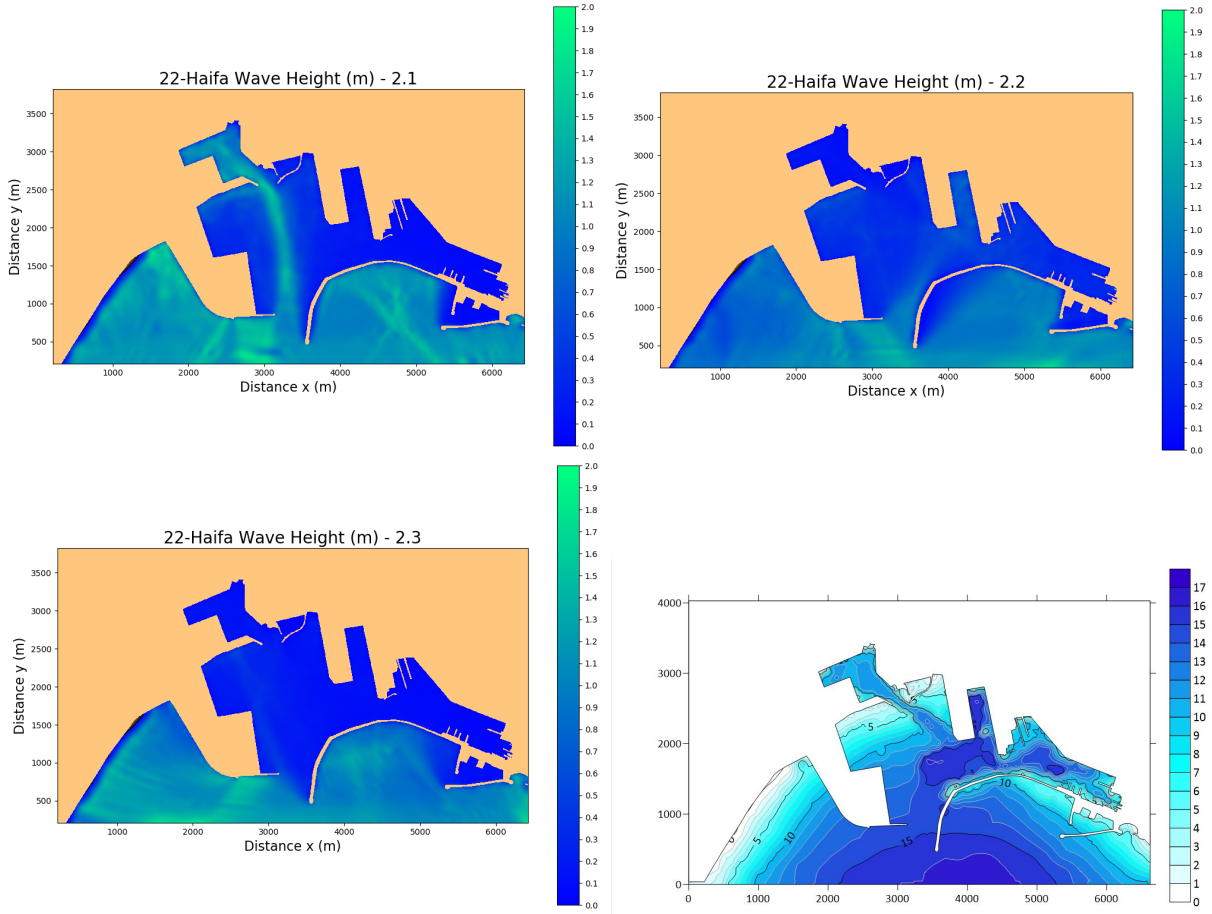

Figure S4.10. Characteristic operational WFS results of Hs (m) by Model B in **Haifa** (Israel; no. 22 of Table 1) port during N, NE and NW sector incoming wind waves and swell of H_s=1m (port orientation is turned 180° clockwise).

Scenarios	**H_s (m)**	**T_p (s)**	**ϕi (˚)**	**t_{sim} (s)**

B#1 (2.1)	1.00	8.00	0	1000
B#2 (2.2)	1.00	8.00	45	1000
B#3 (3.1)	1.00	12.0	0	1000

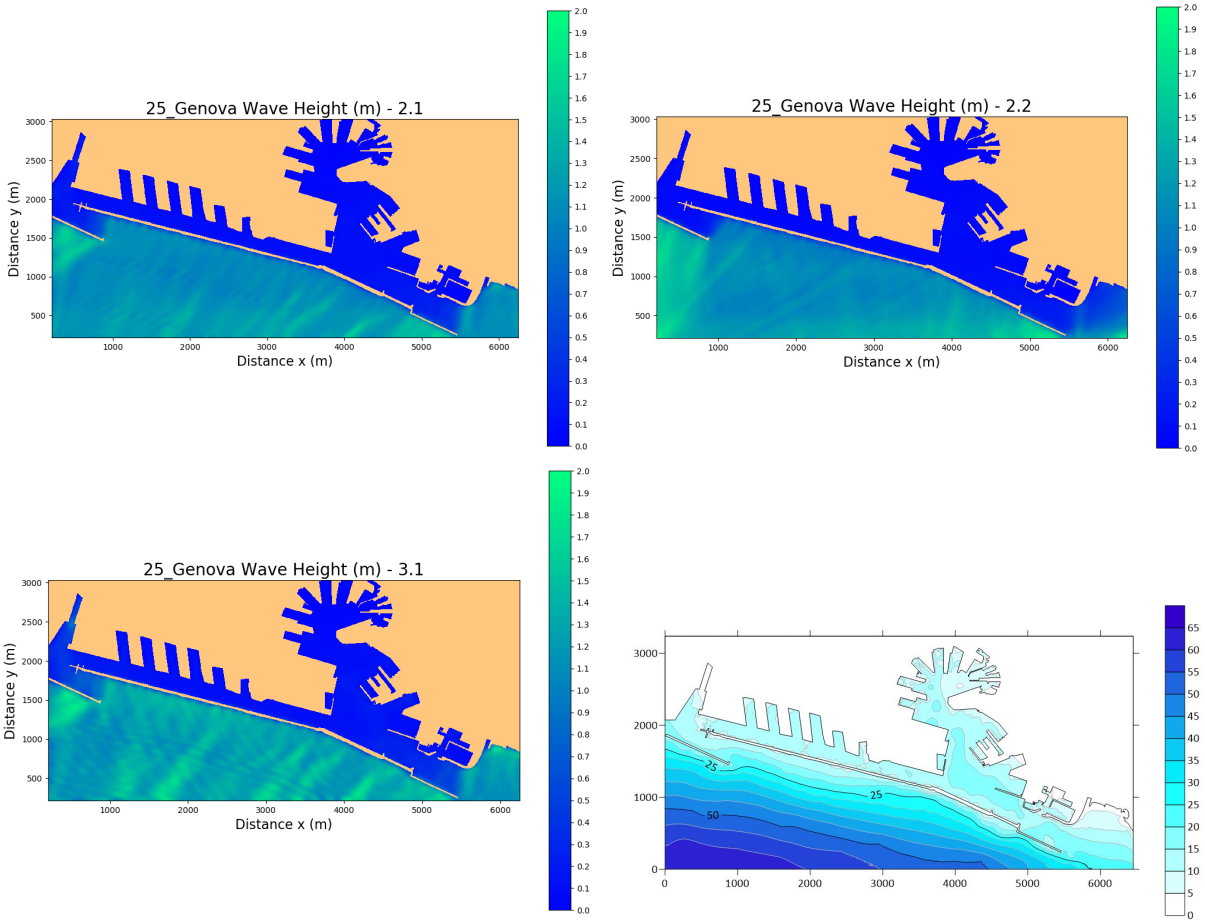

Figure S4.11. Characteristic operational WFS results of Hs (m) by Model B in **Genova** (Italy; no. 25 of Table 1) port during S and SW sector incoming wind waves and swell of H_s=1m.

Scenarios	**H_s (m)**	**T_p (s)**	**ϕi (˚)**	**t_{sim} (s)**
B#4 (3.1)	1.00	12.0	0	1500

B#5 (3.2)	1.00	12.0	45	1500
B#6 (3.3)	1.00	12.0	90	1500

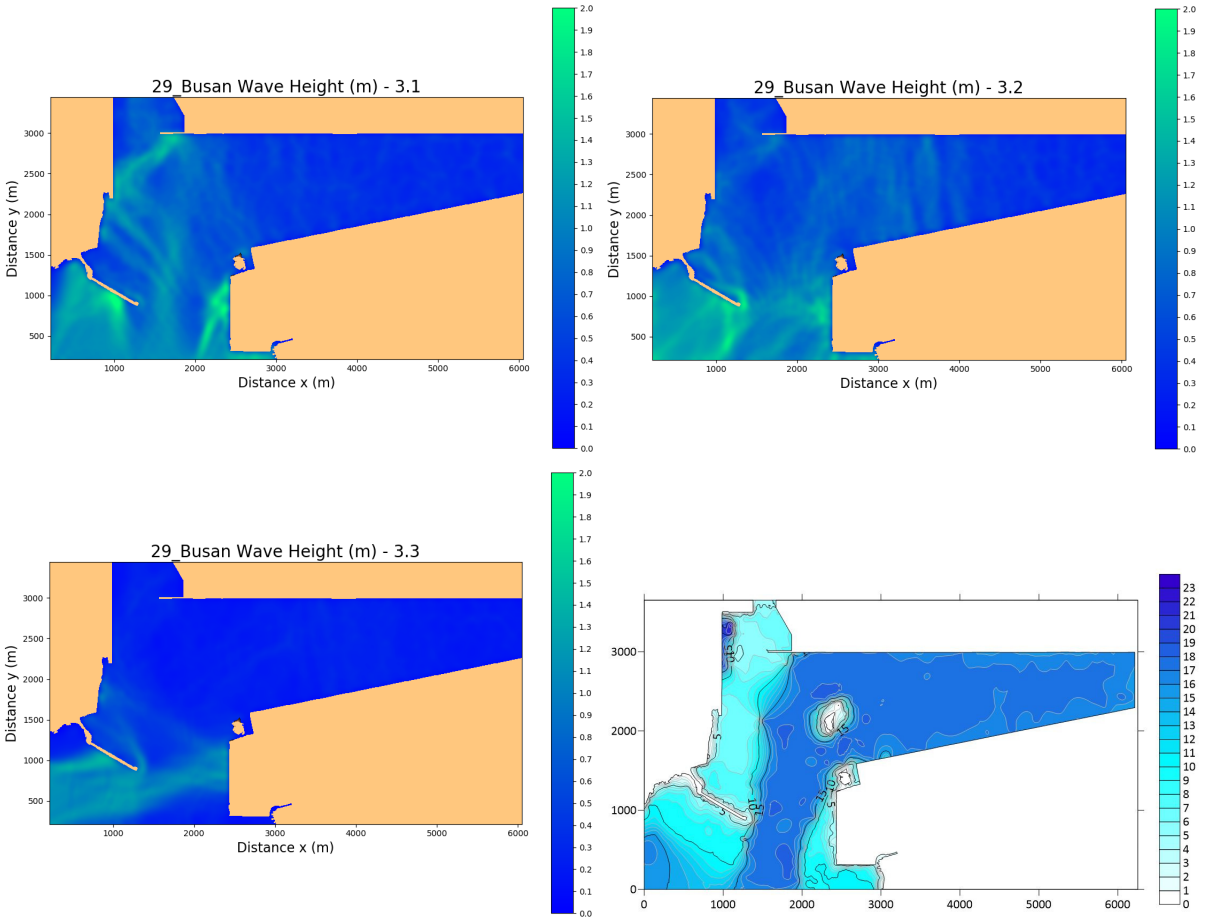

Figure S4.12. Characteristic operational WFS results of Hs (m) by Model B in **Busan** (South Korea; no. 29 of Table 1) new port during S and SW sector incoming wind waves and swell of H_s=1m.

Scenarios	**H_s (m)**	**T_p (s)**	**ϕi (˚)**	**t_{sim} (s)**
B#1 (3.1)	1.00	12.0	180	1100
B#2 (3.2)	1.00	12.0	135	1100

B#3 (3.3)	1.00	12.0	90	1100

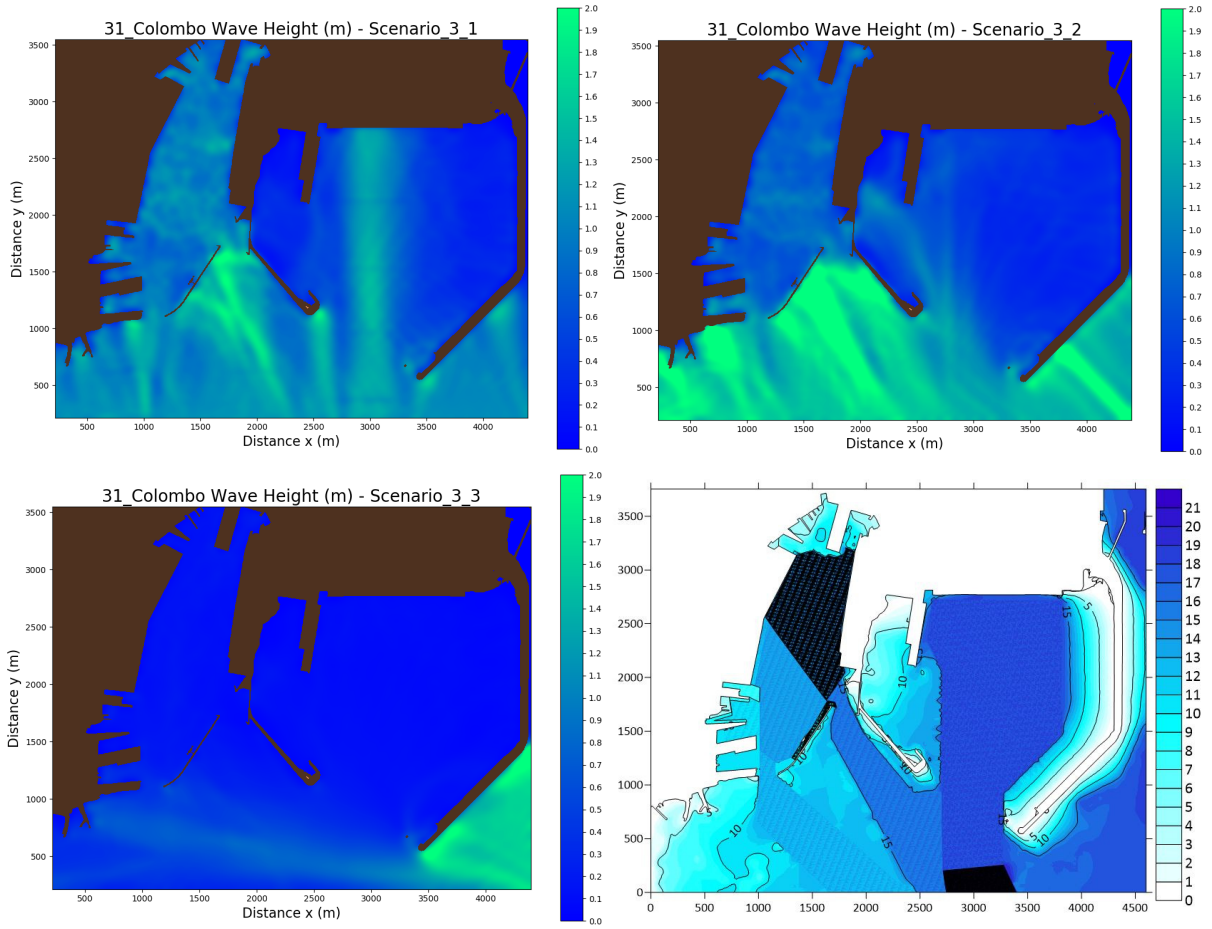

Figure S4.13. Characteristic operational WFS results of Hs (m) by Model B in **Colombo** (Sri Lanka; no. 31 of Table 1) port during N, NW, and W sector incoming wind waves and swell of H_S=1m (port orientation is turned 90° clockwise).

Scenarios	**H_s (m)**	**T_p (s)**	**ϕi (˚)**	**t_{sim} (s)**
B#1 (2.1)	1.00	8.00	180	600
B#2 (2.2)	1.00	8.00	135	600
B#3 (2.3)	1.00	8.00	90	600

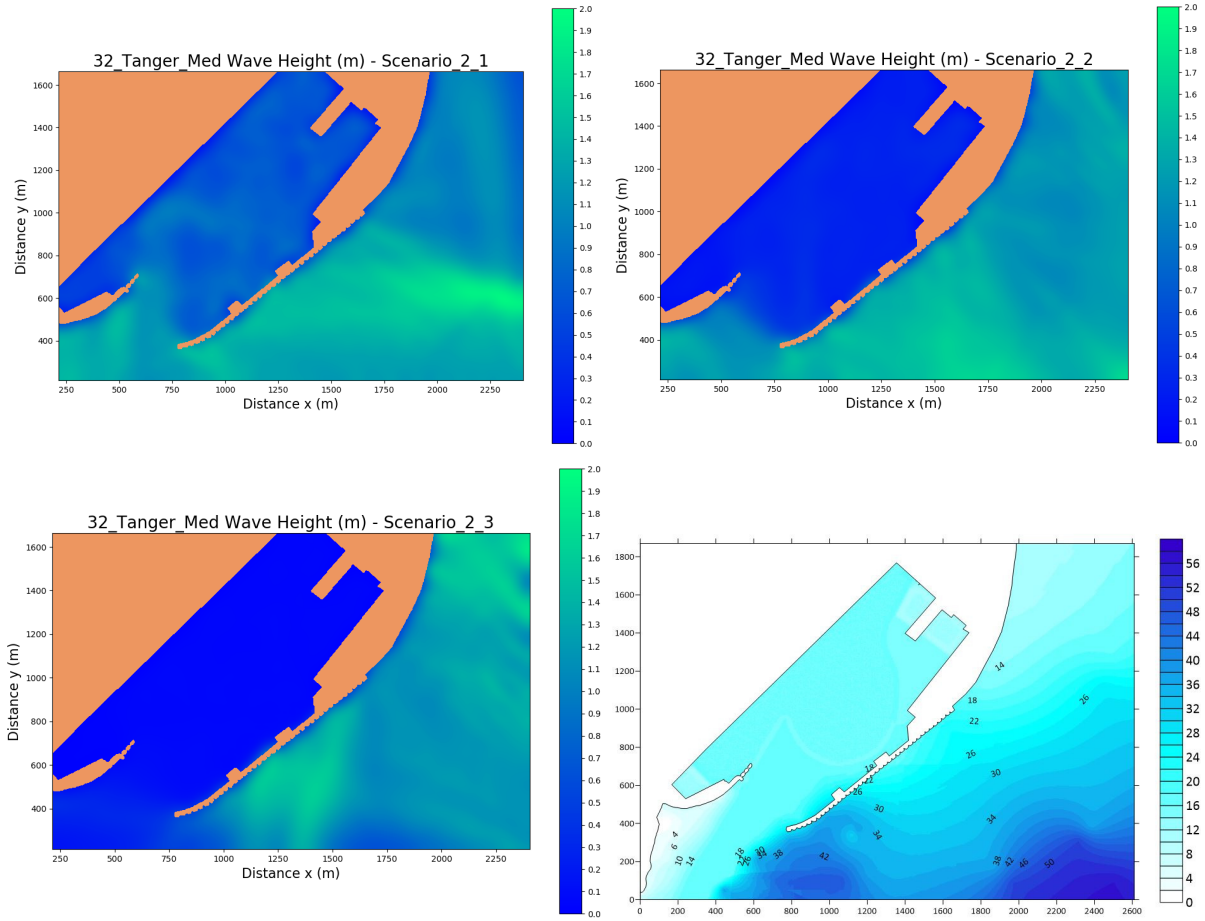

Figure S4.14. Characteristic operational WFS results of Hs (m) by Model B in **Tanger Med** (Morroco; no. 32 of Table 1) port during W, NW, and N sector incoming waves of H_s=1m (port orientation is turned 180° clockwise).

Scenarios	**H_s (m)**	**T_p (s)**	**ϕi (˚)**	**t_{sim} (s)**
B#1 (2.1)	1.00	8.00	90	1100
B#2 (2.2)	1.00	8.00	135	1100
B#3 (2.3)	1.00	8.00	180	1100

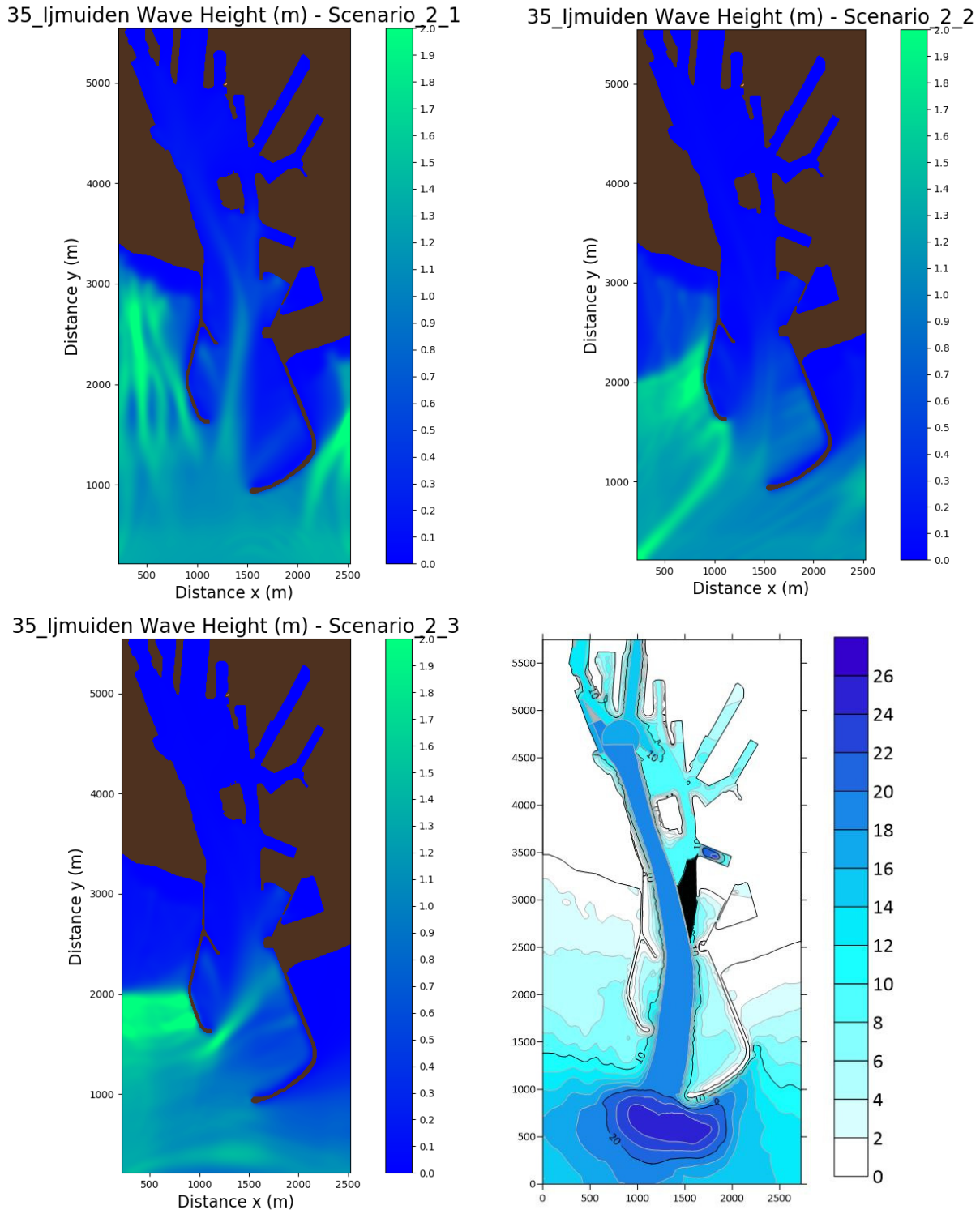

Figure S4.15. Characteristic operational WFS results of Hs (m) by Model B in **IJmuiden** (Netherlands; no. 35 of Table 1) port during W, NW, and N sector incoming waves of H_s=1m (port orientation is turned 180° clockwise).

Scenarios	**H_s (m)**	**T_p (s)**	**ϕi (˚)**	**t_{sim} (s)**
B#1 (3.1)	1.00	12.0	90	800
B#2 (3.2)	1.00	12.0	135	800
B#3 (3.3)	1.00	12.0	45	800

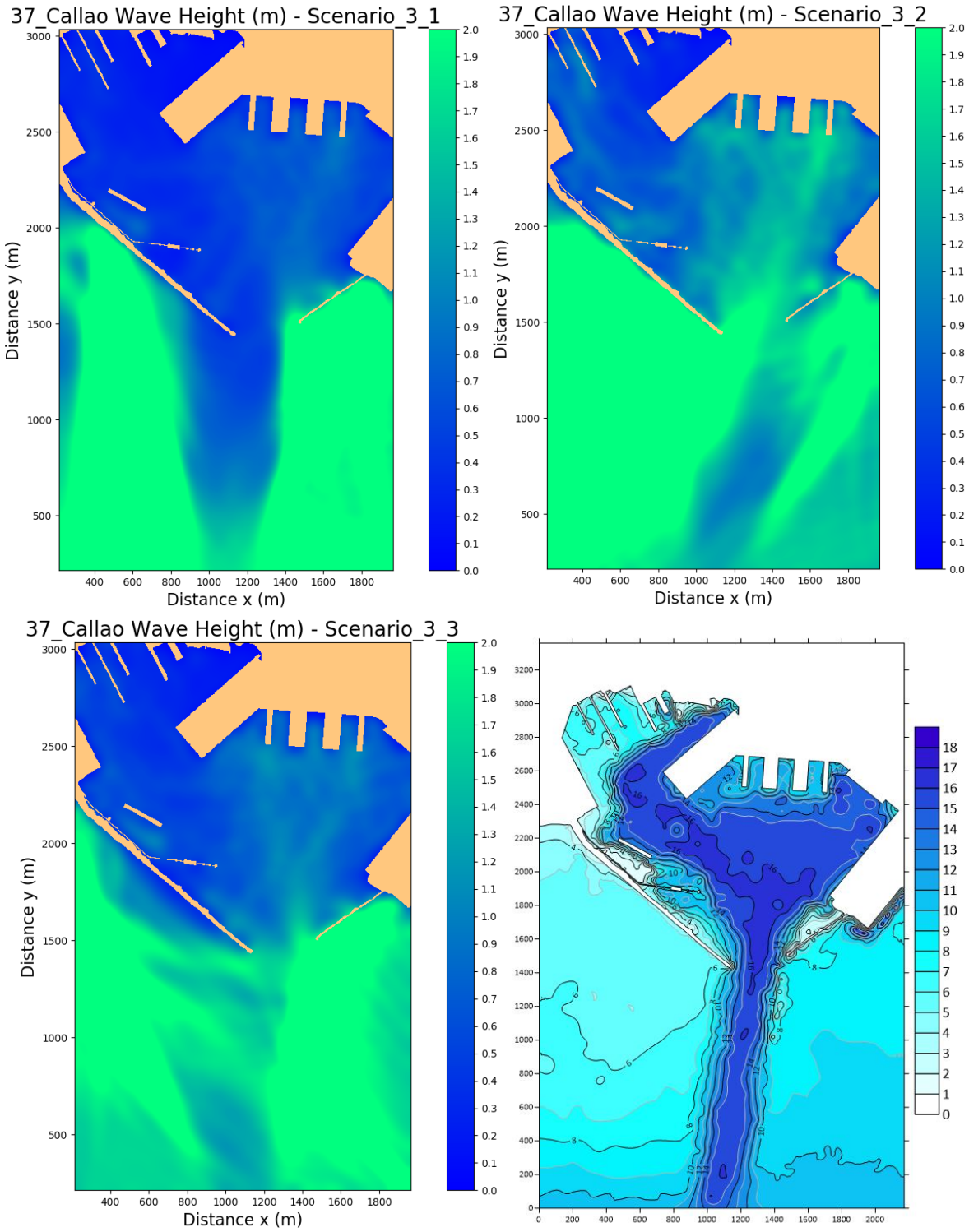

Figure S4.16. Characteristic operational WFS results of Hs (m) by Model B in **Callao** (Peru; no. 37 of Table 1) port during W, NW, and SW sector incoming waves of H_s=1m (port orientation is turned 90° counter-clockwise).

Scenarios	**H_s (m)**	**T_p (s)**	**ϕi (˚)**	**t_{sim} (s)**
B#1 (2.1)	1.00	8.00	0	1100
B#2 (2.2)	1.00	8.00	45	1100
B#3 (2.3)	1.00	8.00	315	1100

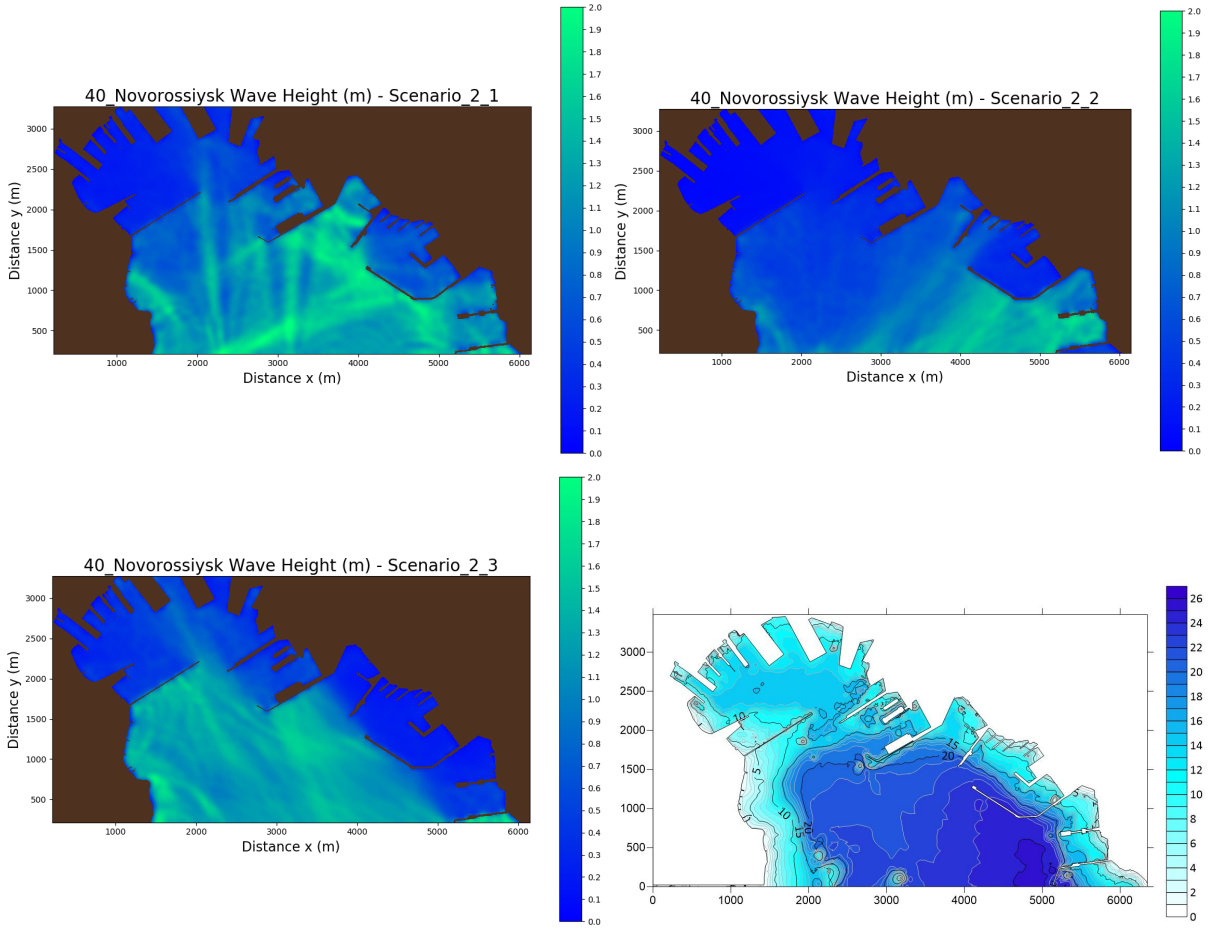

Figure S4.17. Characteristic operational WFS results of Hs (m) by Model B in **Novorossiysk** (Russia; no. 40 of Table 1) port during S, SW, and SE sector incoming waves of H_s=1m.

Scenarios	**H_s (m)**	**T_p (s)**	**ϕi (˚)**	**t_{sim} (s)**
B#1 (2.1)	1.00	8.00	90	1400
B#2 (2.2)	1.00	8.00	135	1400
B#3 (2.3)	1.00	8.00	45	1400

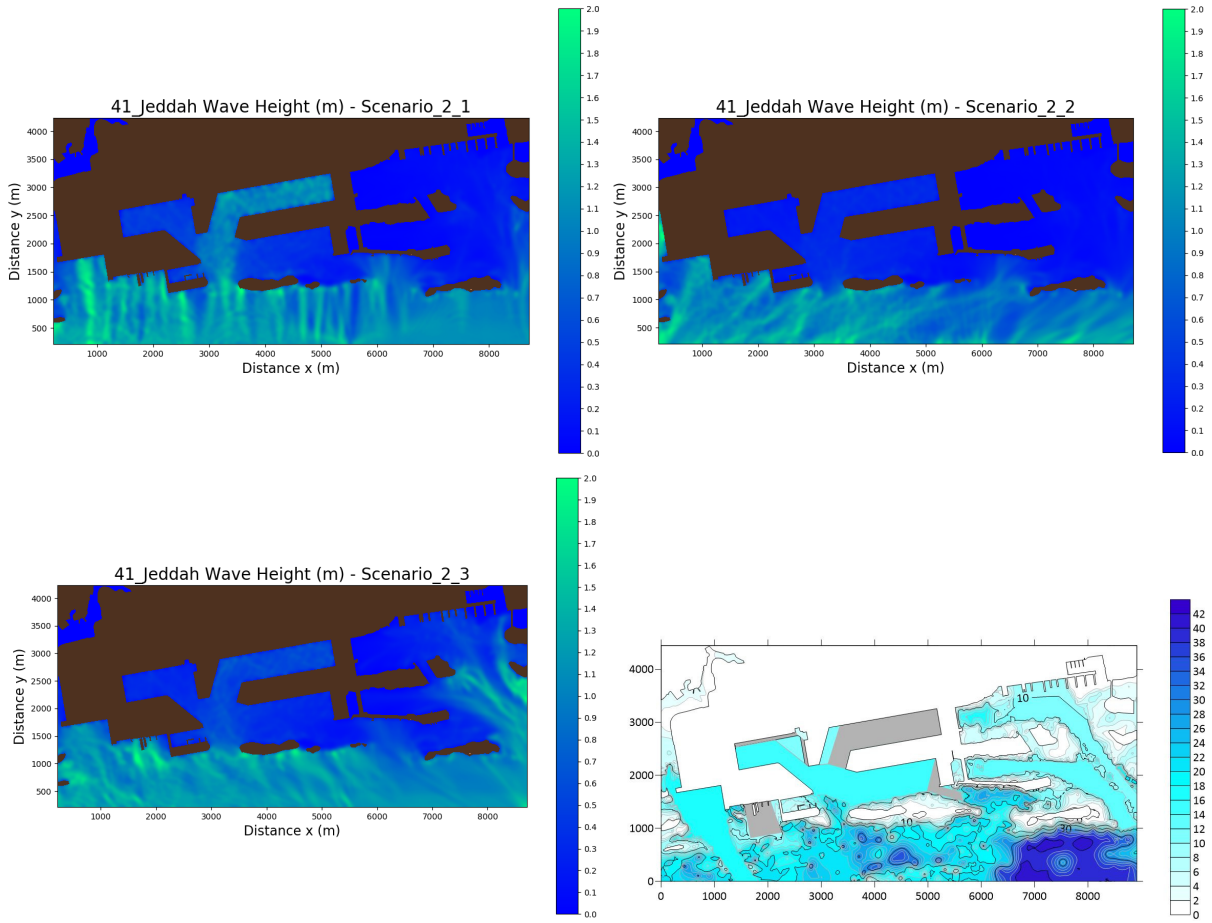

Figure S4.18. Characteristic operational WFS results of Hs (m) by Model B in **Jeddah** (Saudi Arabia; no. 41 of Table 1) port during S, SW, and SE sector incoming waves of H_s=1m (port orientation is turned 90° counter-clockwise).

Scenarios	**H_s (m)**	**T_p (s)**	**ϕi (˚)**	**t_{sim} (s)**
B#1 (2.1)	1.00	8.00	0	700
B#2 (2.2)	1.00	8.00	45	700
B#3 (2.3)	1.00	8.00	315	700

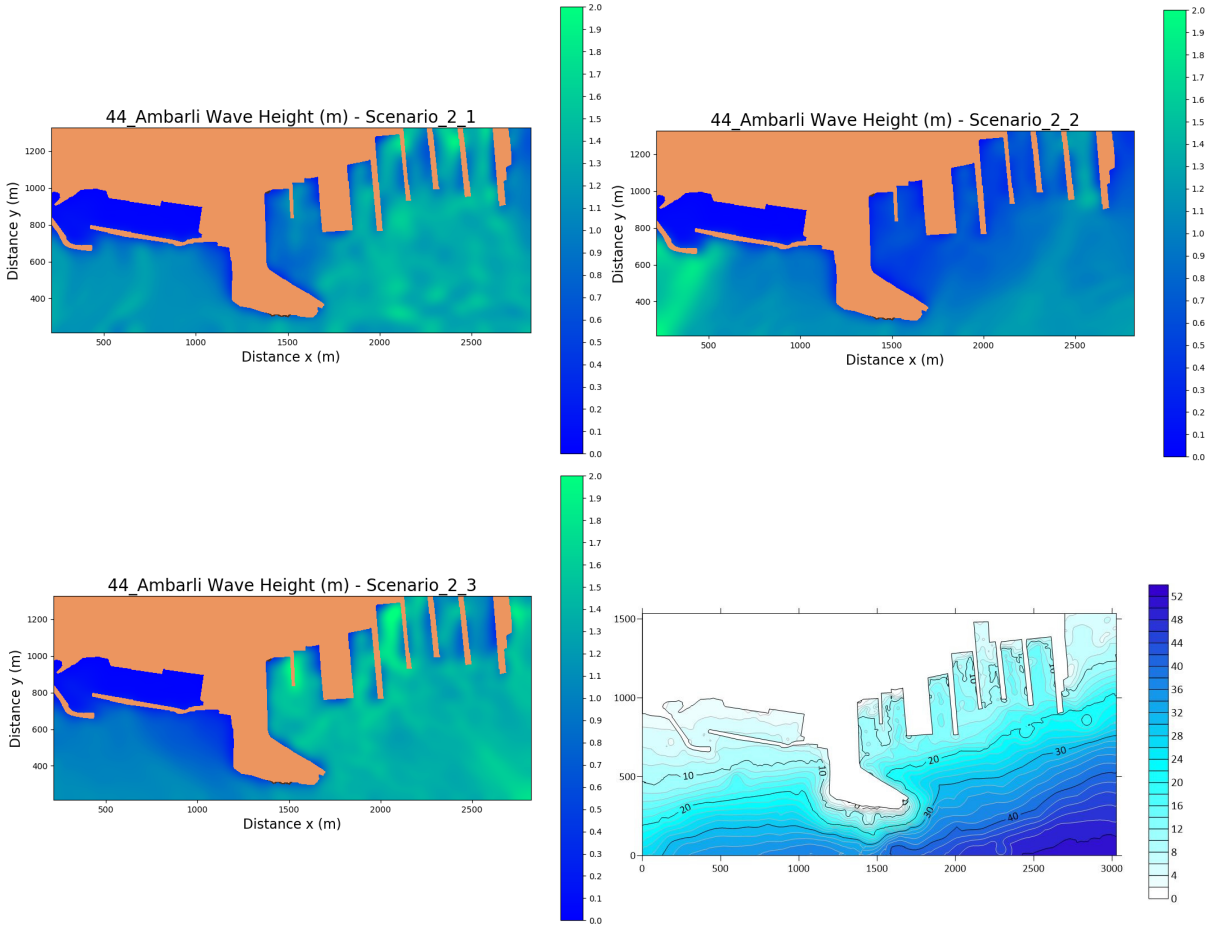

Figure S4.19. Characteristic operational WFS results of Hs (m) by Model B in **Ambarli** (Turkey; no. 44 of Table 1) port during S, SW, and SE sector incoming waves of H_s=1m.

Scenarios	**H_s (m)**	**T_p (s)**	**ϕi (˚)**	**t_{sim} (s)**
B#1 (3.1)	1.00	12.0	180	900
B#2 (3.2)	1.00	12.0	225	900
B#3 (3.3)	1.00	12.0	135	900

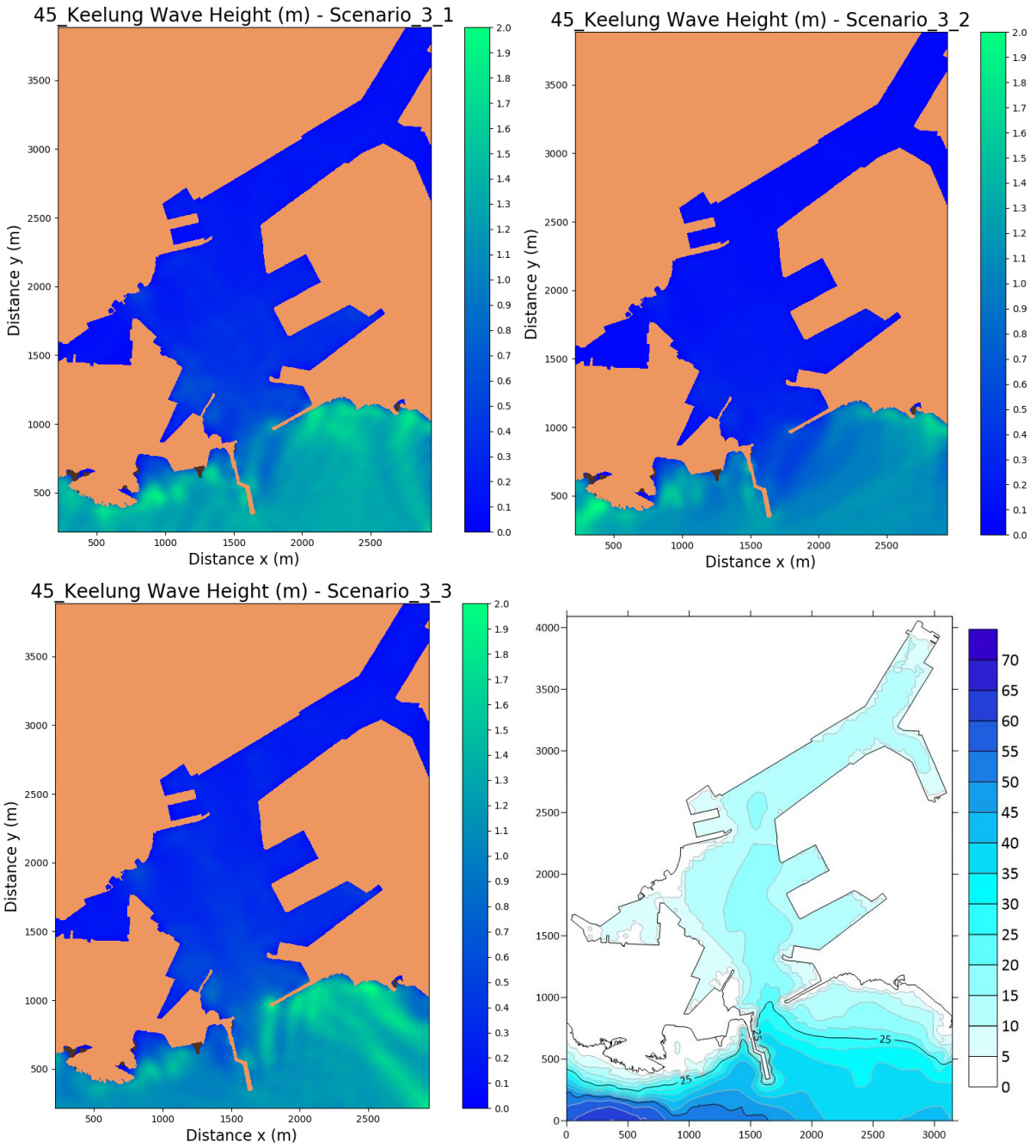

Figure S4.20. Characteristic operational WFS results of Hs (m) by Model B in **Keelung** (Taiwan; no. 45 of Table 1) port during N, NW, and NE sector incoming swell waves of H_s=1m (port orientation is turned 180° clockwise).